T-3785

The Gamma-Ray Reactivities for the p+^{11}B, p+^{6}Li and p+^{7}Li Fusion Reactions and the Applications as Temperature Diagnostics for the Fusion Plasma

By

Huaizhu Liu

T-3785

A thesis submitted to the Faculty and the Board of Trustees of the Colorado School of Mines in partial fulfillment of the requirements for the degree of Master of Science (Physics).

Golden, Colorado
Date: 9/1/89

Signed: 刘怀柱 Huaizhu Liu

Huaizhu Liu
Student

Golden, Colorado
Date: 9/1/89

Approved: J E Cecil

Dr. F. E. Cecil
Thesis Advisor

Golden, Colorado
Date: 9/1/89

Signed: F D Schowengerdt

Dr. F. D. Schowengerdt
Physics department Head

Abstract

The gamma ray to alpha particle yield ratios for the $p+^{6}Li$, $p+^{7}Li$,and $p+^{11}B$ fusion reactions, which were recently measured by the nuclear physics group at CSM on the charged particle accelerator (E(lab)=40-180keV), are used to deduce the astrophysical S-factors. The gamma reacitivies for those fusion reactions are calculated for plasma temperature up to kT=50 keV and the application of the gamma reactivities as temperature diagnostics for a fusion reactor is discussed.

Table of Contents

List of Figures

List of Tables

Acknowledgements

I would like to sincerely appreciate Professor Ed Cecil for his thoughtful guidance. His encouragement and patience made this work possible.

I would also like to appreciate Dr. James McNeil, my committee chairman, for his comments on the original version of this thesis.

I would like to thank Abdelkader Outzourhit and John Scorby for the helpful discussions on this thesis.

I would also like to thank the Physics Department, the Graduate School, and the U.S. Department of Energy for their financial support (U.S. DOE Contracts #DE-FG02-87ER 40342 and #DE-FG02-88ER 53276).

I would like to thank my host family here in Golden, Mr. and Mrs. Johnson, for their kindness and friendship.

My special thanks to my wife and my daughter for the strength they gave to me.

Finally, I am grateful to all those that have taught and helped me in my academic career.

Chapter I. Introduction

The fossil-fuel reign will probably present only a short interlude, as sketched in Fig. I-1. Three reasons are responsible: 1) The amount of fossil fuel is limited; 2) It is irreplaceable; 3) It produces substantial pollution (FR74). To satisfy growing energy needs, scientists and engineers have continually sought safer, more economical and more plentiful sources of energy.

High among the candidates of new energy sources is nuclear power. It has been known for many years that energy may be released by modifying the structure of certain atomic nuclei. One well-known method is the process of fission during which the release of energy results from the splitting of heavy nuclei into lighter fragments. An alternative and potentially much more important method is the process of fusion: a considerable amount of energy will be produced when certain very light nuclei are combined into heavier components (BI58).

Fission reactors possess two shortcomings: they produce a large amount of hazardous nuclear waste, and they lead to heat pollution (FR74).

In contrast to the case of fission, a fusion reactor would present no problem of disposal of radioactive waste.

And the fusion reactor fuels are quite plentiful. For example, the total amount of deuterium, which is the fuel for D+D or D+T fusion reaction, on the earth is estimated to be about 10^{17} pounds. It may provide a source of energy for some twenty thousand million years! Moreover, the cost of this fuel is relatively low(BI58).

A fusion reaction is initiated if two light nuclei are brought to such a high temperature that the kinetic energy is sufficient to overcome the Coulomb barrier, the long range electrostatic repulsion between the reaction mixture. The energy which nuclei require to fuse together corresponds to a very high temperature at which the gas atoms are fully ionized and form a plasma. For instance, a deuterium nucleus undergoes fusion with a tritium nucleus when their relative kinetic energy is larger than 4.5 keV (TE81). To achieve a energy like this, a temperature of near 100 million degrees Kelvin is needed, since 10 keV approximately corresponds to 10^8 degrees Kelvin.

There are three conditions which must be satisfied for a self-sustaining fusion reaction (FR74): the plasma must be raised to the required temperature (ignition point), the plasma density must be proper, and temperature and density must be maintained for a sufficiently long time (adequate confinement). In table I-1, several fusion reactions are

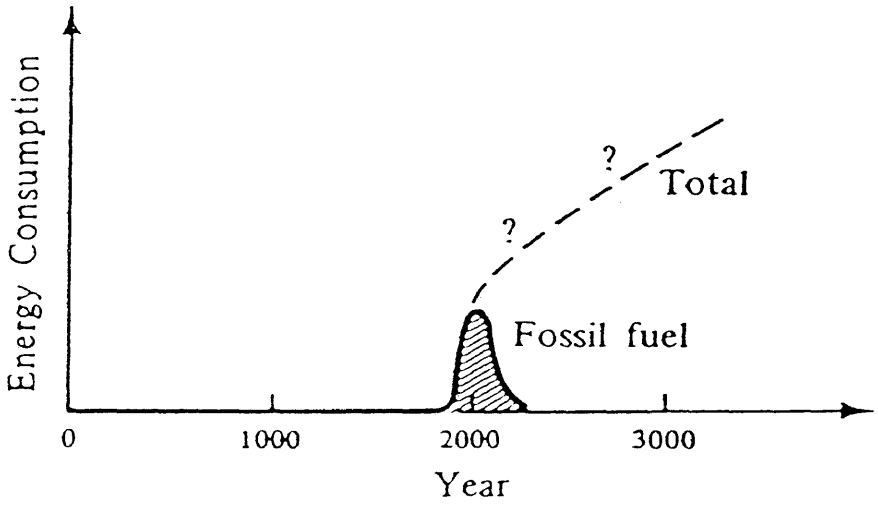

Fig.I-1. Short reign of fossil fuel (FR74).

listed and some of cross sections for those reactions are shown in Fig.I-2.

Table I-1

Some fusion reaction with released energies (FR74)

$D+D=^{3}He+n+4.0$ MeV

$D+D=T+p+3.25$ MeV

$D+T=^{4}He+n+17.6$ MeV

$D+^{3}He=^{4}He+p+18.3$ MeV

It is very important to know the plasma temperature as accurately as possible since it indicates how near a self-sustaining fusion reaction is to ignite for a given fuel density and confinement time.

Several diagnostic techniques have been used to measure plasma temperature: the ion temperature can be determined by measuring neutrons emitted from thermonuclear reactions, infrared laser scattering and the Doppler spread in frequency of impurity lines, and the electron temperature can be founded by probing magnetic bremsstrahlung or synchrotron radiation (MA79 and WH79).

Some fusion reactions may produce monoenergetic gamma

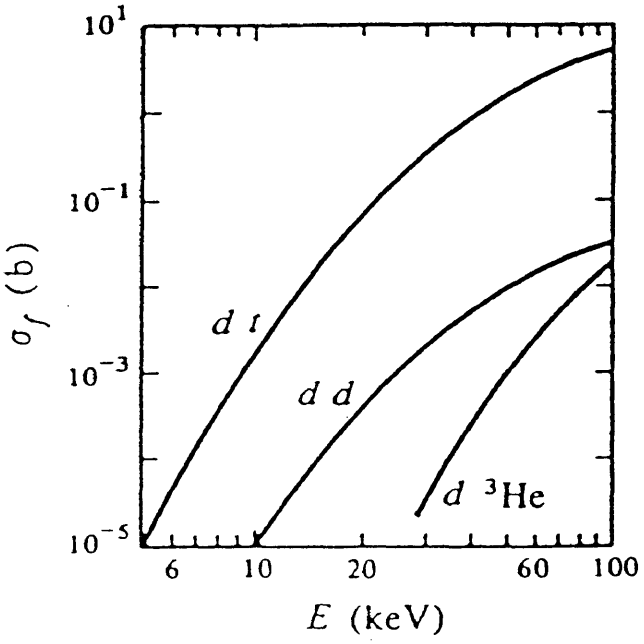

Fig.I-2. Cross sections for the fusion reactions as a function of the deuteron energy (FR74).

rays with high energy. A list of fusion gamma reactions is given in Table I-2 (ME84).

The concept of gamma rays as fusion temperature diagnostics was first introduced by Medley et al(ME79). An extension of the concept was proposed by Cecil and Newman (CE84) wherein high-resolution gamma ray spectroscopy was applied to obtain ion temperature measurements in Maxwellian Plasma. The first observation of 5.5 MeV gamma rays from the D(p,gamma)^{3}He reaction was completed by Newman and Cecil during hydrogen neutral beam heating of a deuterium plasma in Doublet-III (NE84).

The quantity relevant for energy prodution is the reactivity which is the product of the cross section for the reaction and the relative velocity of the colliding partners, averaged over the Maxwellian distribution of the positive ions in the plasma at a high temperature (TE81). A detailed discussion of the reactivity is given in Appendix A. The reactivity $\langle\sigma v\rangle$ is related to the equilibrium plasma temperature through the Maxwellian velocity distribution of interacting particles. If one multiplies $\langle\sigma v\rangle$ with the product of the densities of the two colliding partners, one gets the reaction rate which is the number of reactions per unit volume per unit time. Therefore, the plasma temperature

Table.I-2

Fusion gamma reactions (ME84)

Reaction	Gamma-ray energy (MeV)
$p+D=\gamma+{}^{3}He$	5.5
$p+T=\gamma+{}^{4}He$	19.7
$D+D=\gamma+{}^{4}He$	23.8
$D+T=\gamma+{}^{5}He$	16.7
$D+{}^{3}He=\gamma+{}^{5}Li$	16.4
$D+{}^{4}He=\gamma+{}^{6}Li$	1.5
$T+T=\gamma+{}^{6}He$	12.3
$T+{}^{3}He=\gamma+{}^{6}Li$	15.8
$T+{}^{4}He=\gamma+{}^{7}Li$	2.5
${}^{3}He+{}^{3}He=\gamma+{}^{6}Be$	11.5
${}^{4}He+{}^{3}=\gamma+{}^{7}Be$	1.6
$P+{}^{7}Li=\gamma+{}^{8}Be$	18.0 and 15.0
$P+{}^{11}B=\gamma+{}^{12}C$	16.1 and 11.7 and 4.4

is linked to the reaction rate via the reactivity and can be determined by measuring the reaction rate.

Since the fuel D+T can be ignited at the a low temperature of about 5 keV, it is the easiest one by far to be able to sustain a thermonuclear reaction. However, the D+T fuel has number of drawbacks. First, the amount of tritium on earth is very small and it has to be produced artificially; Secondly, problems like the activation of the surrounding environment and the structural damage associated with neutron production of the D+T reaction are serious; Finally, careful handling of radioactive tritium adds greatly to the expense of a reaction device (DA81).

One of the main advantages for using the so called advanced fuels is that they yield no or much fewer neutrons than D+T fuel. Consequently, the problems associated with neutron production can be minimized. Some of possible advanced fuel candidates are listed in Table I-3. As an example, we will briefly discuss the advantage of $p+^{11}B$ if it were used as an advanced fuel. Since the abundance of both boron and hydrogen is very large, $p+^{11}B$ meets our need to have an economical energy source. The $p+^{11}B$ reaction produces no neutrons. Therefore, $p+^{11}B$ has been considered as an attractive candidate for practical fusion fuels, although it requires a relatively high temperature (about

Table.I-3

Some advanced-fuel reactions and side reactions (DA81)

$P+{}^{11}B=3{}^{4}He+8.7$ MeV

$P+{}^{6}Li={}^{3}He+{}^{4}He+3.865$ MeV

${}^{3}He+{}^{6}Li=2{}^{4}He+P+16.6$ MeV

${}^{6}Li+{}^{6}Li=3{}^{4}He+20.5$ MeV

${}^{3}He+D={}^{4}He+n+18.2$ MeV*

${}^{3}He+{}^{9}Be=3{}^{4}He+18.74$ MeV

$D+{}^{6}Li=P+{}^{7}Li+4.9$ MeV

$={}^{7}Be+n+3.3$ MeV**

$={}^{4}He+T+P+2.5$ MeV

$={}^{4}He+{}^{3}He+n+1.7$ MeV***

$=2{}^{4}He+22.0$ MeV

* run 90%${}^{3}He$, 10%D

** Maximum neutron energy-2.89 MeV

*** Maximum neutron energy-1.5 MeV

300 keV) for a sustained fusion reaction (DA81).

In this thesis, we focus on the studies of three advanced-fuel fusion reactions: $p+^{11}B$, $p+^{6}Li$ and $p+^{7}Li$.

In Chapter II, the gamma ray to charged particle branching ratio technique is applied to determine the astrophysical S-factors of the gamma branches for those fusion reactions.

In Chapter III, the gamma S-factors obtained in Chapter II are used to calculate the gamma reactivities and the application of the reactions as a fusion plasma thermometer is discussed.

Chapter II. S-factors

1) Introduction

As pointed out in Chapter I, reactivity $\langle\sigma v\rangle$ is a velocity weighted integral of the cross section over the Maxwellian distribution. The cross section can also be written as (RO78):

$$\sigma(E) = \frac{S(E)}{E} e^{-b/\sqrt{E}} \qquad \text{(II-1)}$$

where S(E) is the so-called astrophysical S-factor which is the nuclear structure part of the cross section; b is the Summerfeld parameter characterizing the reaction by the charge of the reactants and their relative velocity (see Appendix A).The S-factor is connected to the reactivity through the expression (II-1). Obviously, the reactivity $\langle\sigma v\rangle$ can be calculated if the S-Factor is known. So, determining the S-factors for the interested reactions is our task in this Chapter.

The detected reaction yield of gamma rays per incident projectile of the energy E_0 in a thick target is (CE87):

$$Y_\gamma(E) = \epsilon_\gamma(E) \int_{E_0}^{0} \sigma_\gamma(E) f(E) / (dE(E)/dn)\, dE \qquad \text{(II-2)}$$

where $\epsilon_\gamma(E)$ describes the detector efficiency and solid

angles; dE(E)/dn is the stopping power for the target. The relevant stopping powers are given by Ziegler (ZE77); f(E) is the fractional density of target atoms at the incident proton energy E_0. f(E) may be assumed to be constant in the energy range of our measurement (40-180 keV).

Similarly, the detected reaction yield of alphas is given by:

$$Y_\alpha(E) = \epsilon_\alpha(E)\int_{E_0}^{0}\sigma_\alpha(E)f(E)/(dE(E)/dn)dE \qquad \text{(II-3)}$$

Dividing (II-2) by (II-3), we can get the yield ratio as follows:

$$\frac{Y_\gamma}{Y_\alpha} = \frac{\epsilon_\gamma(E)\int\sigma_\gamma(E)f(E)/(dE(E)/dn)dE}{\epsilon_\alpha(E)\int\sigma_\alpha(E)f(E)/(dE(E)/dn)dE} \qquad \text{(II-4)}$$

The cross section of alpha particle reaction is related to that of the gamma reaction by the branching ratio (CE84):

$$\frac{\sigma_\gamma(E)}{\sigma_\alpha(E)} = \frac{\Gamma_\gamma}{\Gamma_\alpha} \qquad \text{(II-5)}$$

Replacing $\sigma_\gamma(E)$ by the product of the branching ratio and $\sigma_\alpha(E)$ in equation (II-4), we can express the yield ratio as follows:

$$\frac{Y_\gamma}{Y_\alpha} = \frac{\epsilon_\gamma(E)\int(\Gamma_\gamma/\Gamma_\alpha)\sigma_\alpha(E)f(E)/(dE(E)/dn)dE}{\epsilon_\alpha(E)\int\sigma_\alpha(E)f(E)/(dE(E)/dn)dE} \qquad \text{(II-6)}$$

Under the assumption that the branching ratio $(\Gamma_\gamma/\Gamma_\alpha)$ is independent of energy, it may be factored out of the

integral expression for Y_γ in (II-6) and then,

$$\frac{Y_\gamma}{Y_\alpha} = \frac{\epsilon_\gamma(E)}{\epsilon_\alpha(E)} \frac{\Gamma_\gamma}{\Gamma_\alpha} \qquad \text{(II-7)}$$

Combining (II-1), (II-5) and (II-7), we may establish the relationship between the S-factors and the yield ratios:

$$\frac{S_\gamma}{S_\alpha} = \frac{Y_\gamma}{Y_\alpha} \frac{\epsilon_\alpha(E)}{\epsilon_\gamma(E)} \qquad \text{(II-8)}$$

If we express the cross section in terms of S-factor and differentiate both sides of (II-4), we have:

$$S_\gamma = S_\alpha y + \frac{\int S_\alpha e^{-b/\sqrt{E}}/E(dE/dn)dE}{e^{-b/\sqrt{E}}/E(dE/dn)}(dy/dE) \qquad \text{(II-9)}$$

where

$$y = (Y_\gamma/Y_\alpha)(\epsilon_\alpha(E)/\epsilon_\gamma(E)) \qquad \text{(II-10)}$$

is the yield ratio of the detected gamma ray to the alpha particle, including the detector efficiencies and the solid angles; dy/dE is the first derivative of the yield ratio with respect to the proton energy. The yield ratios are known from the measurements accomplished by the Nuclear Physics Research Group at Colorado School of Mines Physics Department. The measurements have been carried out on the General Ionex Model 1545 low energy, high current particle accelerator between proton lab energies of about 40 to 180 keV on the thick target (CE88). dy/dE can be found from the yield ratios. Additionally, the S-factors for the dominant

alpha branches were determined by other physicists. Then, from (II-9), we can get several measured values of the gamma S-factors for the studied capture reactions.

From these measured branching ratios, we can use three different methods to estimate the gamma ray S-factors:

i) If the yield ratios for the gammas and alphas are approximately constant, from (II-8), the ratios can be used to determine the gamma S-factors without knowing the details of the stopping power and the density of the target atoms.

ii) In case of resonant reaction, the gamma S-factor is assumed to have a specific form characterized by some parameters. In light of the peak value, the parameter related to the resonant term can be determined first and the rest of the parameters can be easily fitted by using the least-square method.

iii) The third method is the direct use of the least-square analysis to determine the coefficients for the appropriately chosen bases.

2). $p+^{11}B$

The cross section for the $^{11}B(p,3\alpha)$ reaction has been measured by Davidson et al (DA79) for the lab energies from 35.4 to 1500 keV. When the center-of-mass energy is less than 522 KeV, the S-factor has been deduced to be

(see Fig.II-1):

$$S_\alpha = 160+400E^2+1.11x10^{-2}/(E-.1498)^2+7.29x10^{-6}) \quad (II-11)$$

The units of the center-of-mass energy are MeV and those of S are MeV-b. For the resonance at 163 keV (lab system), the resonance cross section was measured to be 5.2±0.6 mb and the resonance S is 1690±50 MeV-b.

The decay schemes of the gamma branches for the $p+^{11}B$ reaction are shown in Fig.II-2 (CE88).

The measurements of the gamma ray to alpha particle yield ratios for the transitions indicated in Fig.II-2 have been completed by the CSM nuclear physics group on the charged particle accelerator. The results are shown in Fig.II-3 and Table II-1 (CE88).

i) Since the yield ratios are strongly dependent on energy, this method is not applicable for the determination of the gamma S-factors.

ii) For $p+^{11}B$ reaction, the stopping power is (ZE77),

$$dE/dn = S(low)S(high)/(S(low)+S(high)) \quad (II-12)$$

Where,

$$S(low) = 2.815E \text{ (keV/cm)} \quad (II-13)$$

$$S(high)=(1206/E)Ln(1+(1060/E)+.02855xE) \text{ (keV/cm)} \quad (II-14)$$

To be able to use the equation (II-9) to derive the measured values for the gamma S-factors, the derivatives of the yield ratios are neccessary to be found . For each yield

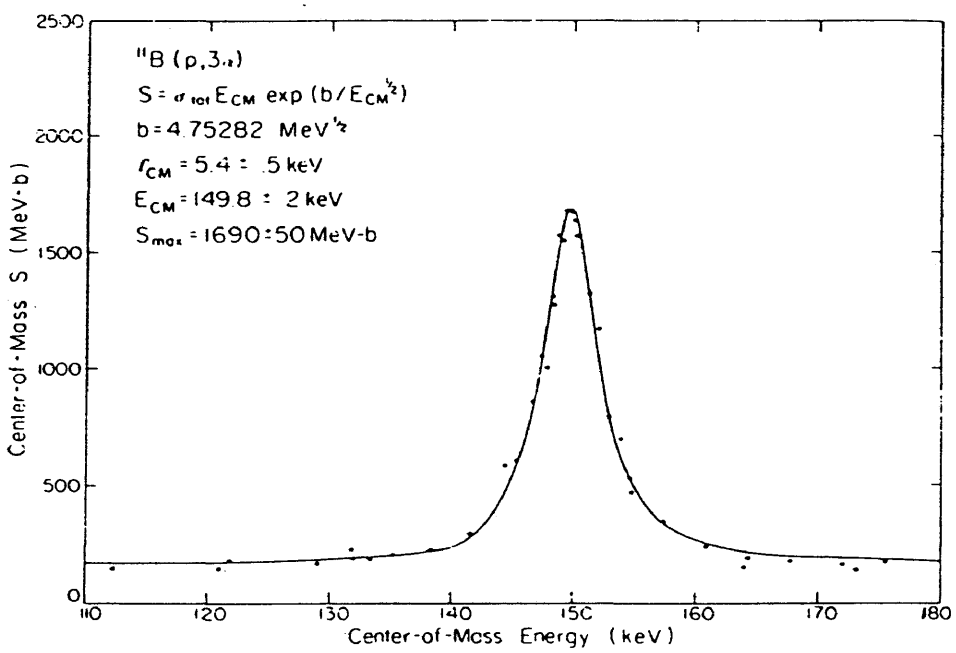

Fig.II-1. S-factor in the neighborhood of the 150 kev (c.m.) resonance in ^{11}B(p,3alphas). The solid curve is an empirical fit (DA79).

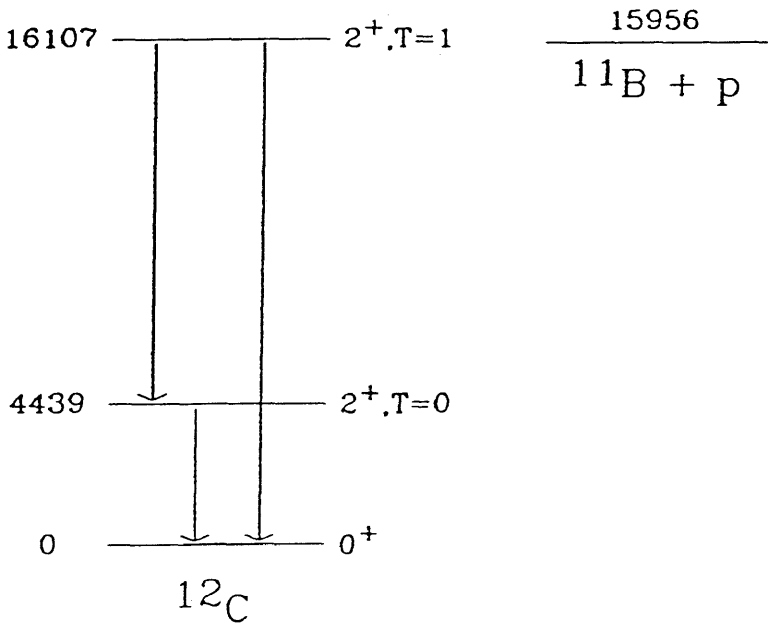

Fig. II-2. Energy levels and decay schemes for the $^{11}B(p,gamma)^{12}C$ reactions (CE88).

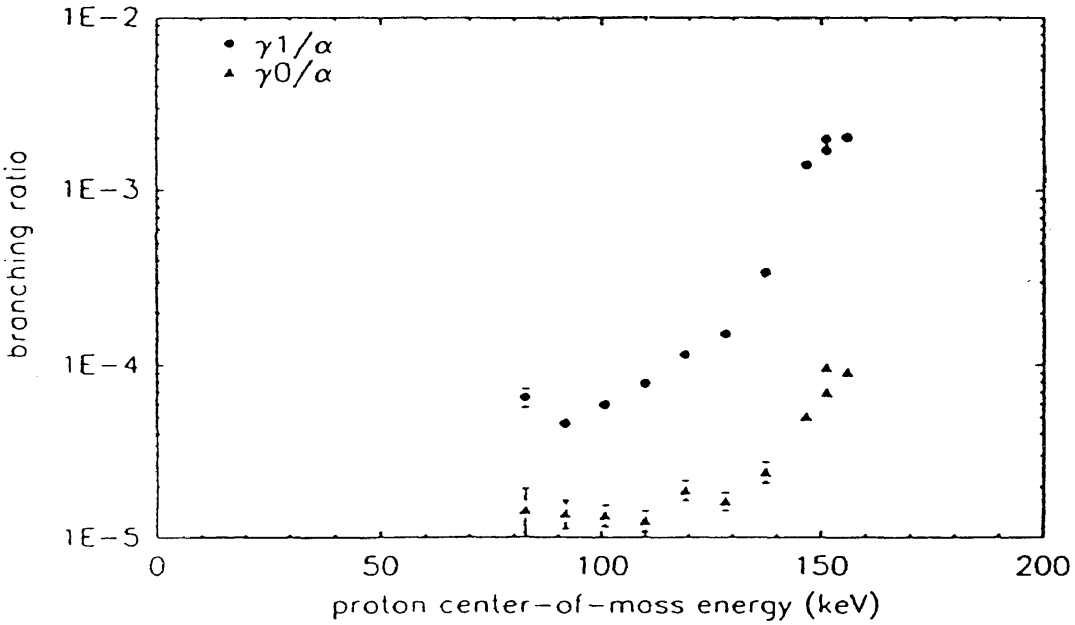

Fig.II-3. Yield ratios for the p+^{11}B reaction (CE88).

Table II-1

Yield ratios for $p+^{11}B$ (CE88)

E (c.m. keV)	gamma1	gamma0
82	$6.5\pm.5(x10^{-5})$	$1.46\pm.5(10^{-5}$
92	$4.6x10^{-5}$	$1.4\pm.25(x10^{-5})$
101	$5.96x10^{-5}$	$1.36\pm.2(x10^{-5})$
110	$7.9x10^{-5}$	$1.26\pm.2(x10^{-5})$
119	$1.15x10^{-4}$	$1.91\pm.2(x10^{-5})$
128	$1.52x10^{-4}$	$1.65\pm.2(x10^{-5})$
138	$3.4x10^{-4}$	$2.43\pm.2(x10^{-5})$
147	$1.4x10^{-4}$	$5.06x10^{-5}$
151	$1.86x10^{-4}$	$8.36x10^{-5}$
156	$2.04x10^{-3}$	$9.16x10^{-5}$

ratio, its derivative is obtained by dividing the difference between this ratio and that of its nearest neighbor by the energy inteval. The results are presented in Table II-2.

We put quantities like alpha S-factor S_α, the stopping power dE(E)/dn, the yield ratio y and the slope of the yield ratio dy/dE into (II-9) and notice that the parameter b for this reaction is 4.75 $(MeV)^{1/2}$, the derived values of the gamma S-factors are plotted in Fig.II-4 and Fig.II-5.

Compared with the alpha S-factor, it is understandable that the S-factor should also have a resonance term since the two branches have the same nature.

For $^{11}B(p,gamma1)^{12}C$ reaction. The data analysis indicates S(gamma1) should have the following form:

$$S(gamma1)=A+BE+C/((E-.15)^2+7.29x10^{-6}) \quad (MeV-b) \qquad (II-15)$$

Since S(gamma1) at the resonance is approximately 100 times larger than the off resonance terms, it is sufficient for the resonance S(gamma1) to have a simple form by ignoring the off-resonance terms:

$$S(gamma1)=C/(7.29x10^{-6}) \qquad (II-16)$$

On the other hand, at resonance, dy/dE is equal to zero.

From (II-9), we have:

$$y=S(gamma1)/S(alpha) \qquad (II-17)$$

Substituting (II-17) into (II-16), the parameter C can

Table II-2

Derivatives of Yield Ratio for $p+^{11}B$

E (keV) (c.m.)	dY/dE (1/keV) (gamma1)	dY/dE (1/keV) (gamma0)
92	1.5×10^{-6}	-4.4×10^{-8}
101	2.2×10^{-6}	-1.1×10^{-7}
110	4.0×10^{-6}	7.2×10^{-7}
119	4.1×10^{-6}	-2.9×10^{-7}
128	1.9×10^{-5}	7.8×10^{-7}
138	1.2×10^{-4}	2.9×10^{-6}
147	1.2×10^{-4}	8.3×10^{-6}
151	3.6×10^{-5}	8.3×10^{-6}
156	3.7×10^{-4}	1.6×10^{-6}

be estimated:

$$C = (7.29\times10^{-6})S(\text{alpha})y$$
$$= (7.29\times10^{-6})\times1690\times1.86\times10^{-3}$$
$$= 2.29\times10^{-5}\ ((\text{MeV}^3\text{-b}) \qquad \text{(II-18)}$$

The off-resonance parameters A and B can be determined by using the least-square fitting:

$$A = -.05 \quad (\text{Mev-b}) \qquad \text{(II-19)}$$

$$B = .75 \quad (\text{b}) \qquad \text{(II-20)}$$

So, the explicit form of S(gamma1) is:

$$S(\text{gamma1}) = -.05+.75E+2.29\times10^{-5}/((E-.15)^2+7.29\times10^{-6}) \qquad \text{(II-21)}$$

For the $^{11}B(p,\text{gamma0})^{12}C$ reaction, we assume that S(gamma0) has a resonance term plus a constant:

$$S(\text{gamma0})=V+W/((E-.15)^2+7.29\times10^{-6}) \quad (\text{MeV-b}) \qquad \text{(II-22)}$$

By the same argument we applied to S(gamma1), the parameter W can be determined immediately:

$$W = (7.29\times10^{-6})S(\text{alpha})y$$
$$= 7.29\times10^{-6}\times1690\times8.36\times10^{-5}$$
$$= 1.19\times10^{-6}\ ((\text{MeV})^3\text{-b}) \qquad \text{(II-23)}$$

For the off-resonance energy range (80-130 keV), S(gamma0) is roughly a constant. The equation (II-10) (S(gamma0)=yS(alpha)) is applicable. Here, $y=1.56\times10^{-5}$ is the average value of the yield ratios in the energy range; S(alpha) is approximately 160 MeV-b. So, we have:

$$V=.0025 \ (\text{MeV-b}) \qquad \text{(II-24)}$$

Then,

$$S(\text{gamma0})=.0025+1.19\times10^{-6}/((E-.15)^2+7.29\times10^{-6}) \quad \text{(II-25)}$$

The fitting results are compared with the experimental data in Table II-4.

iii) We now use the least-square method to deduce the gamma S-factors directly. For S(gamma1), the best fit values for those parameters are:

$$A = -.0516 \text{ (MeV-b)} \quad \text{(II-26)}$$

$$B = .69 \text{ (b)} \quad \text{(II-27)}$$

$$C = 2.71\times10^{-5} \text{ ((MeV)}^3\text{-b)} \quad \text{(II-28)}$$

Then, the fitted equation for S(gamma1) is:

$$S(\text{gamma1})=-.0516+.69E+2.71\times10^{-5}/((E-.15)^2+7.29\times10^{-6}) \quad \text{(II-29)}$$

Even though the results for fitting S(gamma1) from different approaches are close, we realize that method iii) is a more accurate way to fit S(gamma1) than method ii), since the discrepancy between the measured values and the fitted ones is relatively small if we use the least-square method (method iii)).

We keep A and B at best fit values and change the parameter C until the square error $(S(\text{fit})-S(\text{data}))^2$ has a deviation from the best value (minimum value) by an amount of 50%. Then, the range of uncertainty for the parameter C can be determined. The ranges of uncertainty for the off-resonance parameters A and B can be obtained by using

the method for the least-square fitting (YE&CE84).

For S(gamma1):

$\Delta A = .0153$ (MeV-b) (II-30)

$\Delta B = .144$ (b) (II-31)

$\Delta C = 3.26 \times 10^{-6}$ (MeV^3) (II-32)

The least-square-fitted S(gamma1) is plotted in Fig.II-4 and the fitted values are compared with the data points in Table II-3. The fiting curve for S(gamma0) is plotted in Fig.II-5.

Similarly, for S(gamma0), the ranges of uncertainty for the parameters V and W are:

$\Delta V = 9.2 \times 10^{-3}$ (MeV-b) (II-33)

$\Delta W = 2 \times 10^{-7}$ (MeV^3-b) (II-34)

The ranges of uncertainty for S(gamma0) have been determined and shown in Table II-4.

The least-square-fitted result is found to be:

$S(gamma0) = 4.52 \times 10^{-3} + 1.23/((E-.15)^2 + 7.29 \times 10^{-6})$ (II-35)

This expression is not satisfactory since the deviations from the measured values are too large. The reason is that the bases we chose for S(gamma0) are too simple for a good least-square fitting.

Table II-3

S-Factor for $^{11}B(p,gamma1)^{12}C$

E (keV) (c.m.)	S (MeV-b) (data)	S (MeV-b) (fit)
92	$1.07x10^{-2}$	$1.99\pm2.02(x10^{-2})$
101	$1.51x10^{-2}$	$2.93\pm2.12(x10^{-2})$
110	$2.42x10^{-2}$	$4.12\pm2.21(x10^{-2})$
119	$3.28x10^{-2}$	$5.85\pm2.32(x10^{-2})$
128	$9.37x10^{-2}$	$9.19\pm2.49(x10^{-2})$
138	$5.73x10^{-1}$	$2.56\pm.358(x10^{-1})$
147	1.95	$1.71\pm.202$
151	3.22	$3.32\pm.394$
156	.896	$.682\pm.080$

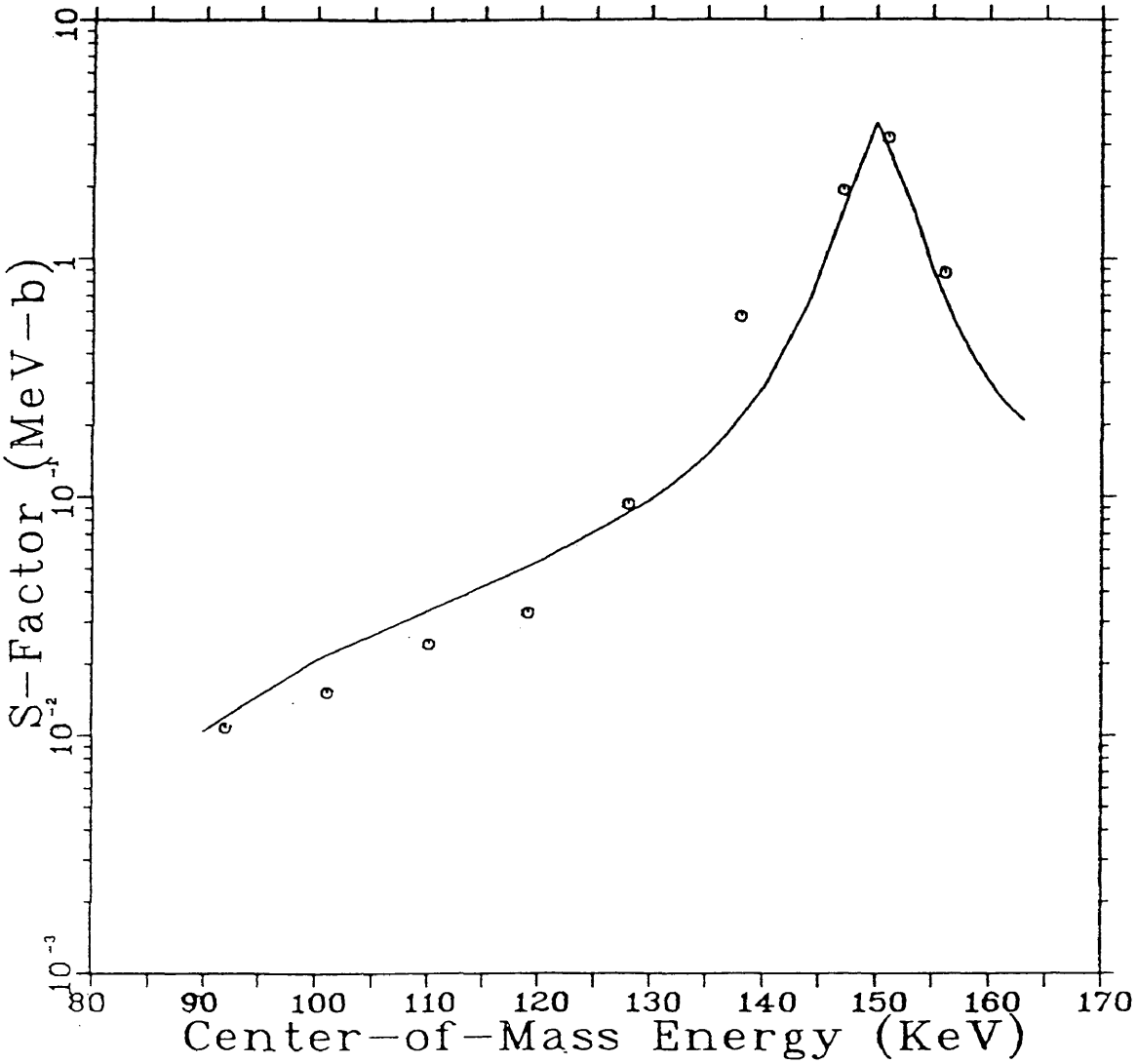

Fig.II-4. S-factor for the $^{11}B(p,gamma1)^{12}C$ reaction. The solid curve is the fitting result.

Table II-4

S-Factor for $^{11}B(p,gamma0)^{12}C$

E (keV) (c.m.)	S (MeV-b) (data)	S(Mev-b) (fit)
82	$2.31\pm.83(x10^{-3})$	$2.76\pm1.35(x10^{-3})$
92	$2.24\pm.42(x10^{-3})$	$2.85\pm1.35(x10^{-3})$
101	$2.04\pm.34(x10^{-3})$	$2.99\pm1.35(x10^{-3})$
110	$4.08\pm.34(x10^{-3})$	$3.24\pm1.36(x10^{-3})$
119	$2.51\pm.35(x10^{-3})$	$3.73\pm1.37(x10^{-3})$
128	$5.82\pm.38(x10^{-3})$	$4.92\pm1.41(x10^{-3})$
138	$1.80\pm.48(x10^{-2})$	$1.04\pm1.90(x10^{-2})$
147	$9.79x10^{-2}$	$7.56\pm1.25(x10^{-2})$
151	$1.44x10^{-1}$	$1.46\pm.245(x10^{-1})$

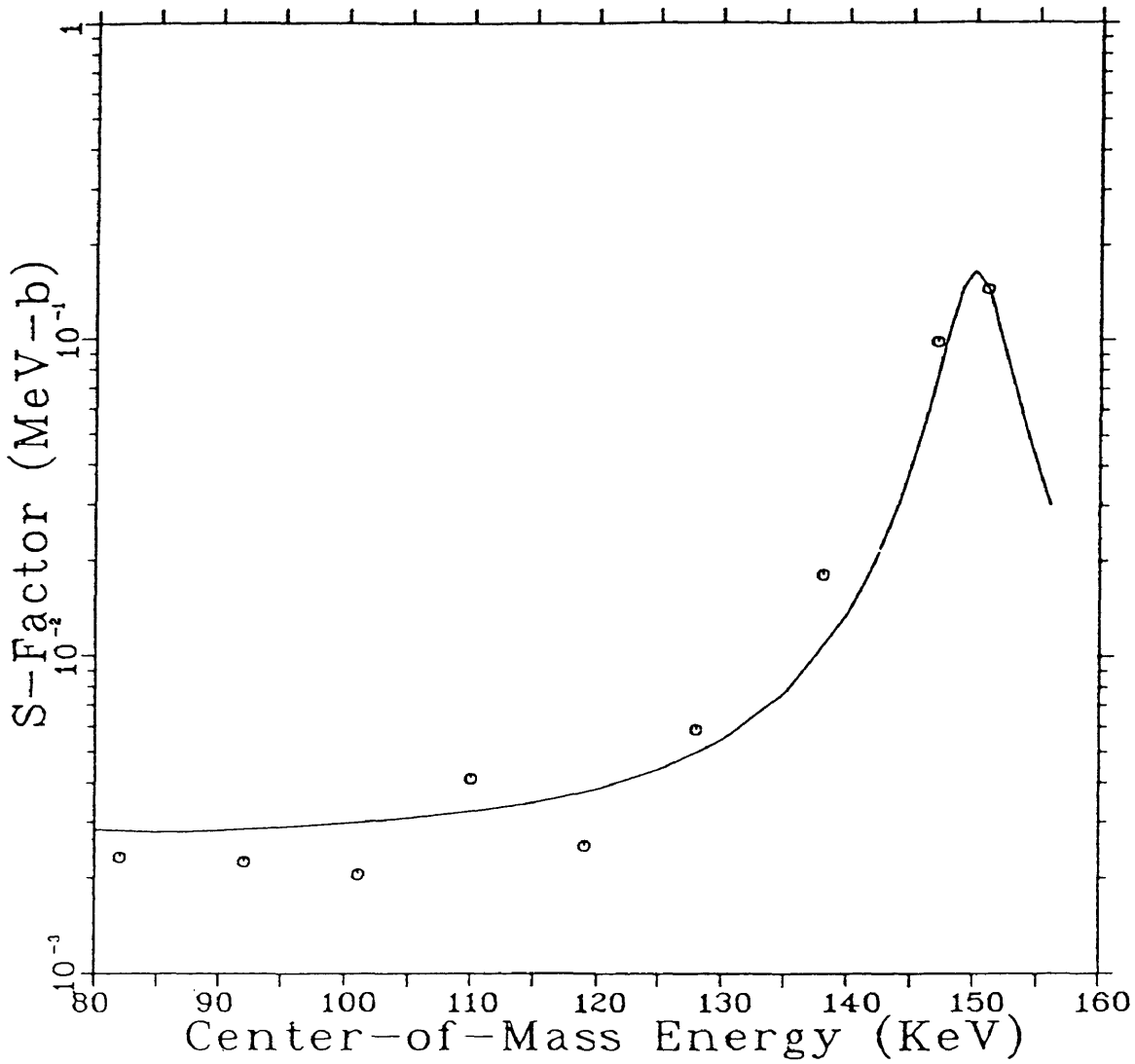

Fig.II-5. S-factor for the $^{11}B(p,gamma0)^{12}C$ reaction. The solid curve is the fitting result.

3) P+^{6}Li

The measurement of the total cross section for the ^{6}Li(p,^{3}He)^{4}He reaction at proton energies between .14 and 3 MeV were performed by Elwyn et al (EL79) at Argonne National Laboratory. The S factor was fitted to:

$$S = 3145(1+(-.0007)E+6x10^{-8}E^{2}) \quad \text{(keV-b)} \qquad \text{(II-36)}$$

Where the units of enegy are keV in the center-of-mass system. The S factor is plotted in Fig.II-6.

The energy level diagram for ^{6}Li(p,gamma)^{7}Be reaction is given in Fig.II-7 (CE88).

The cross section of the reaction ^{6}Li(p,gamma)^{7}Be has been measured by Switkowski et al using Ge(Li) gamma-ray spectrometers for proton bombarding energies from 200 keV to 1200 keV. At E_p=800 keV, the total (p,gamma) integrated cross section is found to be $(3.1\pm.4)x10^{-6}$ b (SW79). Barker's calculation (BA74), supported by the measurements (WA56 and CE88), indicates that the capture gamma-rays populating the ground and first excited states have virtually identical angular distributions.

The yield ratios of the total gamma rays to alpha particle for the p+^{6}Li reaction at proton energies between 40 and 150 keV have been measured by the CSM group and are presented in Fig.II-8 and Table II-5 (CE88).

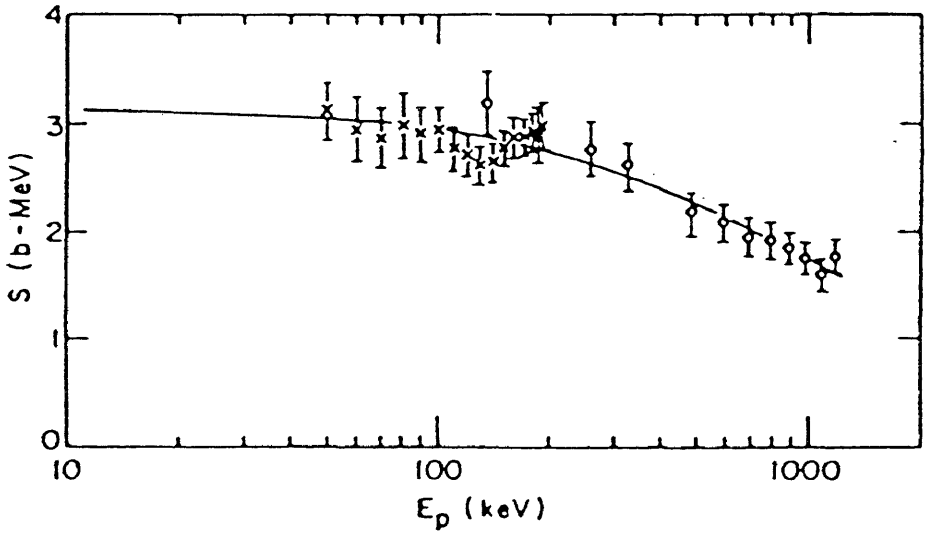

Fig.II-6. Experimental astrophysical S-factor for the $^{6}Li(p,^{3}He)^{4}He$. The solid curve is a least-square fit (EL79).

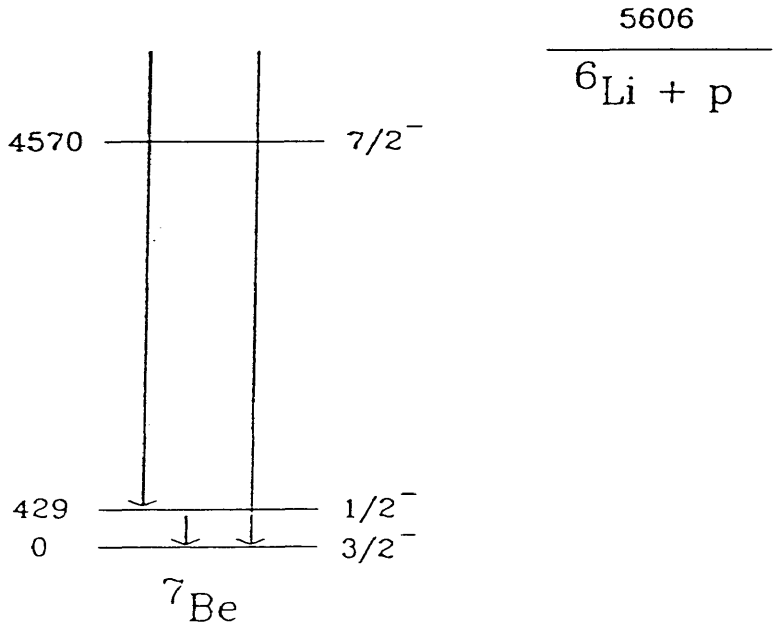

Fig.II-7. Energy levels and decay schemes for the $^{6}Li(p,gamma)^{7}Be$ reaction (CE88).

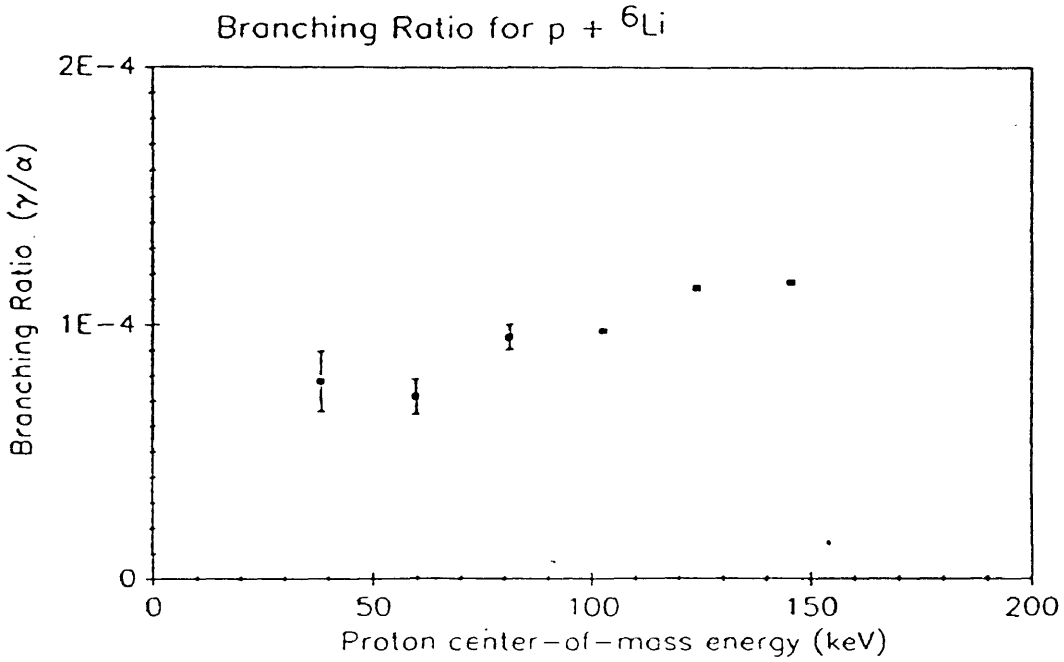

Fig.II-8. Yield ratios for the p+^{6}Li reaction (CE88).

Table II-5

Yield ratios for p+^{6}Li (CE88)

E (c.m. keV)	gamma1+gamma0
38.5	$2.4\pm.40(\times10^{-5})$
60.0	$2.5\pm.30(\times10^{-5})$
81.4	$3.3\pm.17(\times10^{-5})$
103	3.4×10^{-5}
124	3.94×10^{-5}
146	4.10×10^{-5}

i) The average value of the yield ratios is 3.14×10^{-5} and the alpha S-factor can be taken to be 3145 (keV-b). From (II-8), the gamma S-factor cna be estimated as follows:

$$S_\gamma = S_\alpha Y(\text{average})$$
$$= 3145 \times 3.14 \times 10^{-5}$$
$$= .099 \quad (\text{keV-b}) \qquad \text{(II-37)}$$

ii) This method is invalid in case of the non-resonant reaction.

iii) As we did for the $p+^{11}B$ reaction, the derivatives of the yield ratios are obtained and listed in Table II-6. The stopping power is:

$$S(\text{low}) = 1.6 \times E^{\cdot 45} \quad (\text{keV/cm}) \qquad \text{(II-38)}$$

$$S(\text{high}) = (725.6/E)\,\text{Ln}(1+(3013/E)+.04578E) \quad (\text{keV/cm}) \qquad \text{(II-39)}$$

and the constant b for this reaction is 87 $(\text{keV})^{1/2}$. From (II-9), some measured values for the S(gamma) within the energy range of our experiment are derived (see Table II-7).

From the data distribution of the gamma S-factor, we know that it is appropriate to for the S(gamma) to be fitted to a linear expression in the energy range of 40 and 150 keV:

$$S(\text{gamma}) = M+NE \qquad \text{(II-40)}$$

We use the least-square fitting method to determine these parameters. The best values for M and N are:

$$M = .06 \quad (\text{keV-b}) \qquad \text{(II-41)}$$

Table II-6

Derivatives of Yield Ratio for $p+^{6}Li$

E (keV) (c.m.)	dY/dE (1/keV)
38.5	3.10×10^{-8}
60	3.57×10^{-7}
81.4	4.63×10^{-8}
103	2.54×10^{-7}
124	4.53×10^{-8}
146	4.53×10^{-8}

Table II-7

S-Factor for $^{6}Li(p,gamma)^{7}Be$

E (keV) (c.m.)	S (keV-b) (data)	S (keV) (fit)
38.5	.079±.038	.078±.008
60	.072±.023	.081±.008
81.4	.094+.012	.087±.009
103	.095	.096±.010
124	.109	.104±.012
146	.110	.111±.013

$$N = 3.53\times10^{-4} \quad (b) \qquad \text{(II-42)}$$

Thus,

$$S(\text{gamma}) = .06+3.53\times10^{-4}E \qquad \text{(II-43)}$$

The ranges of uncertainties are found by the same fasion as we used for the $p+^{11}B$ reaction:

$$\Delta M = .00705 \quad (\text{keV-b}) \qquad \text{(II-44)}$$

$$\Delta N = 7.31\times10^{-5} \quad (b) \qquad \text{(II-45)}$$

In Table II-7, the fitting results with uncertainties are compared with the experimental data. The fittng curve is plotted in Fig.II-9.

4) $p+^{7}Li$

The total cross section for the reaction $^{7}Li(p,^{4}He)^{4}He$ was obtained by Rolfs and Kavanagh (RO86) from E(c.m.)=25 to 873 keV. The S factor was fitted to:

$$S(\text{alpha})=65(1+1.82\times10^{-3}+2.51\times10^{-6}E^{2}) \ (\text{keV-b}) \qquad \text{(II-46)}$$

Where E is the center-of-mass energy in keV. The resulting S factor curve (Fig.II-10) varies gently with beam energy.

The decay diagram for the gamma reactions is given in Fig.II-11 (CE88).

The thick-target yield ratios of gamma ray to alpha particle accomplished by the CSM group are presented in Fig.II-12 and Table II-8 (CE88).

i) The alpha S-factor is about 65 (keV-b) in the range of

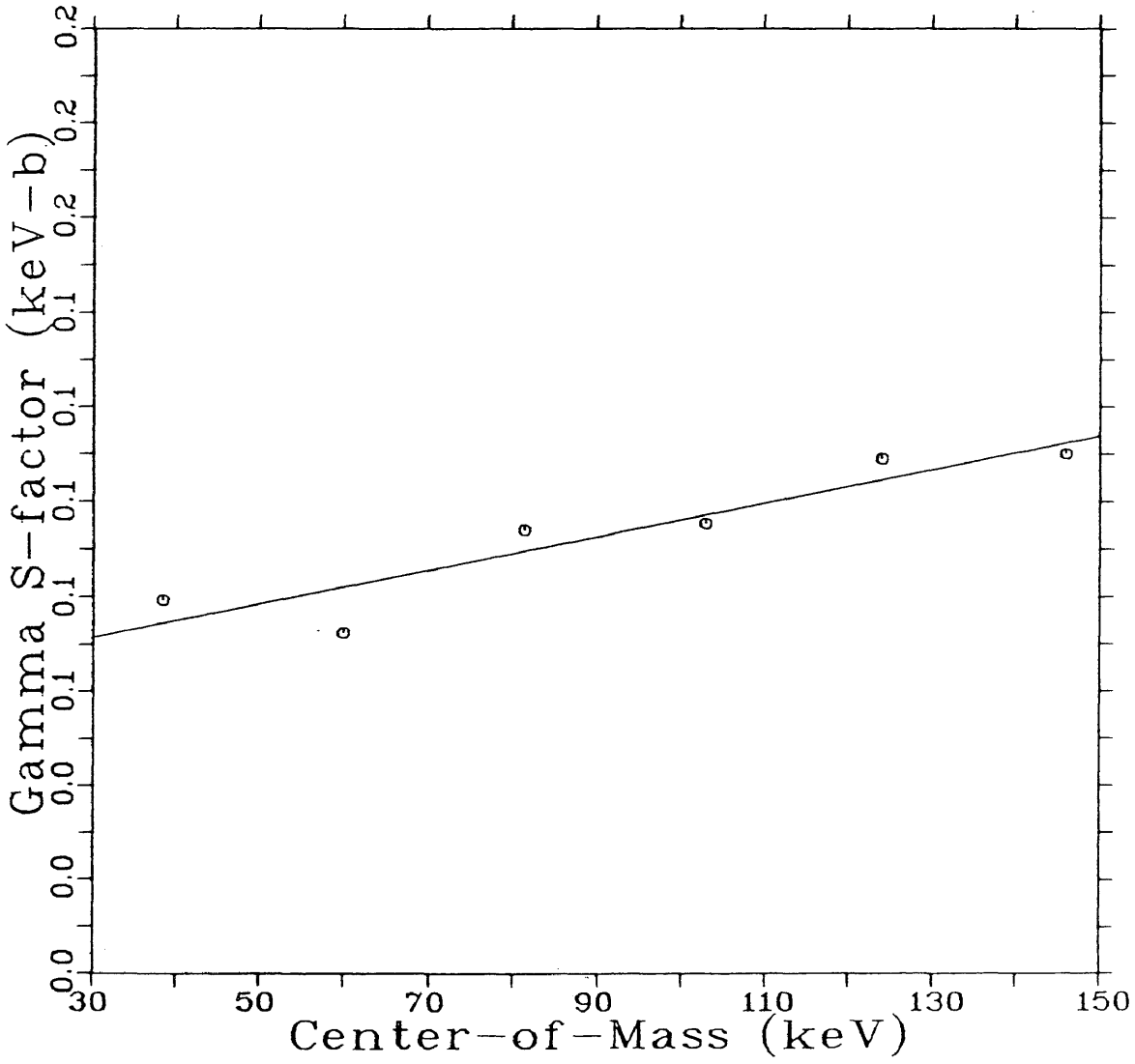

Fig. II-9. S-factor for the $^{6}Li(p,\gamma)^{7}Be$ reaction The solid curve is a least-sqaure fit.

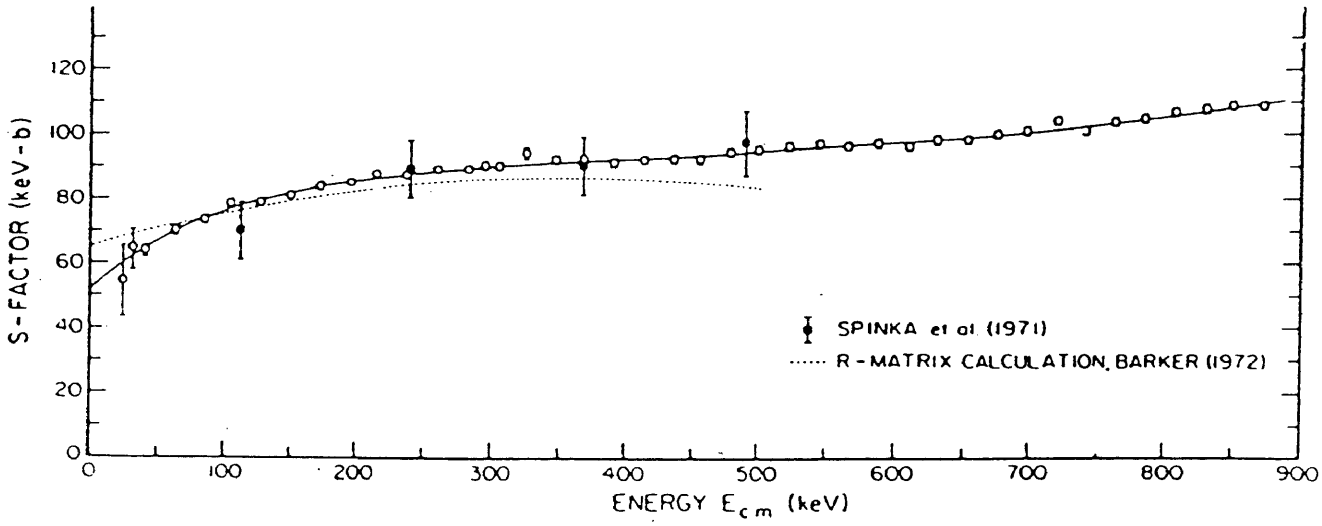

Fig.II-10. S-factor for the $^{7}Li(p,^{4}He)^{4}He$ reaction. The solid line is the fitting result (RO86).

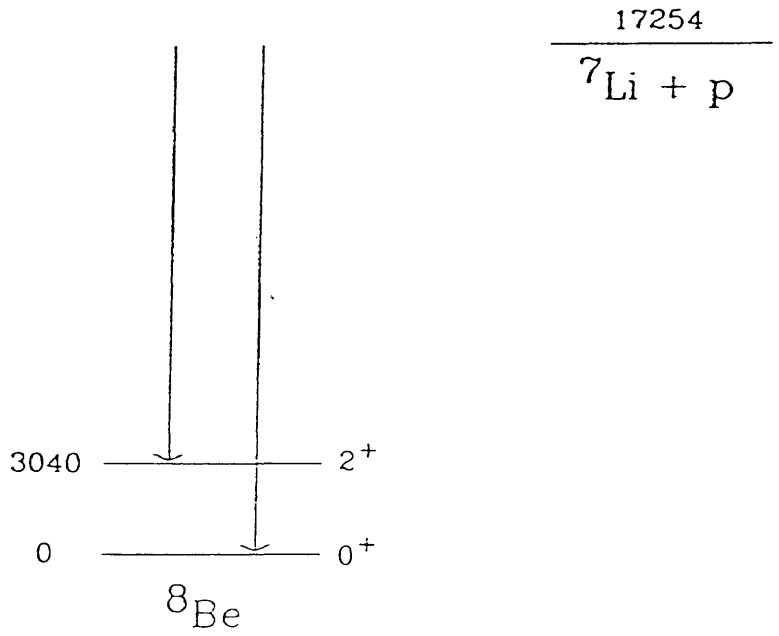

Fig.II-11. Energy diagram and decay schemes for the $^{7}Li(p,\gamma)^{8}Be$ reactions (CE88).

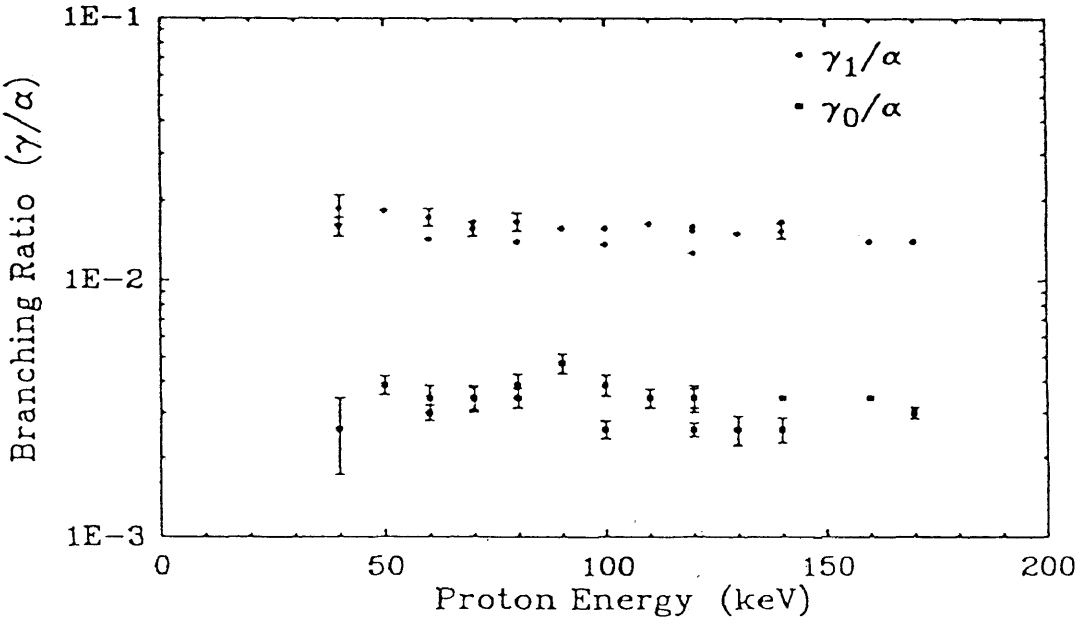

Fig.II-12. Yield ratios for the p+^{7}Li reaction (CE88).

Table II-8

Yield ratios for $p+^{7}Li$ (CE88)

E(c.m. keV)	gamma1	gamma0
34.8	.019±.003	.0026±.0009
52.2	.014	.003±.0006
69.6	.014	.0034±.0006
87	.014	.0026±.00025
104	.016	.0034±.0004
121	.015±.002	.0034
139	.014	.0034
147	.014	.0003±.0002

our measurement.

For S(gamma1), the average yield ratio is .015. The gamma S-factor is:

$$S(\gamma) = S(\alpha)y(\text{avrage})$$
$$= 65 \times .015$$
$$= .975 \ \text{(keV-b)} \qquad \text{(II-47)}$$

For S(gamma0), the average value of the yield ratios is .0031. Thus,

$$S(\gamma_0) = S(\alpha)y(\text{average})$$
$$= 65 \times .0031$$
$$= .202 \ \text{(keV-b)} \qquad \text{(II-48)}$$

iii) The stopping power for the reaction is same as that of the $p+^{6}Li$ reaction. The b parameter is 88 $(kev)^{1/2}$. The derivatives of the yield ratios are listed in Table II-9. By the same way we dealt with the $p+^{11}B$ and $p+^{6}Li$ reactions, from (II-9), the measured values of the gamma S-factors are calculated and the data points are shown in Fig.II-13.

Within the energy range of our experiment, it is proper to assume that the S-factors for the gamma ray branches are constants.

By using the least-square fitting, the best fit values for the S(gamma1) and S(gamma0) with the ranges of uncertainty are found to be:

Table II-9

Derivatives of Yield Ratio for $p+^{7}Li$

E (keV) (c.m.)	dY/dE (1/keV)	dY/dE (1/keV)
34.8	-5.7×10^{-5}	2.3×10^{-5}
52.2	0	2.3×10^{-5}
69.6	0	-4.6×10^{-5}
87	1.2×10^{-4}	4.7×10^{-5}
104	-5.9×10^{-5}	0
121	-5.6×10^{-5}	0
139	0	-2.2×10^{-5}
147	0	-2.2×10^{-5}

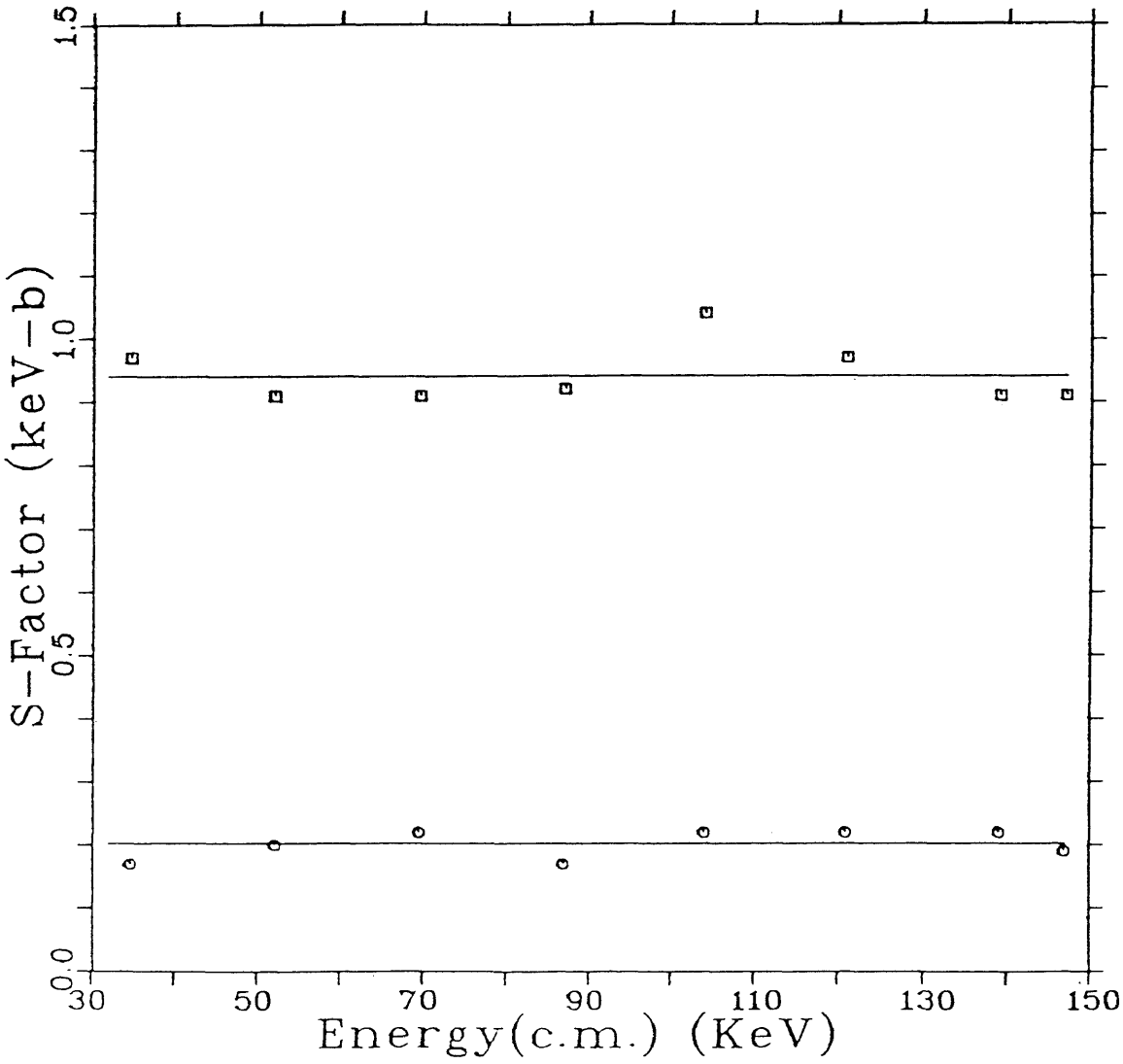

Fig.II-13. The gamma S-factors for the p+^{7}Li reactions. The upper is for the S(gamma1) and the lower is for the S(gamma0).

$$S(\text{gamma1}) = .94 \pm .03 \quad (\text{keV-b}) \qquad \text{(II-49)}$$

And,

$$S(\text{gamma0}) = .202 \pm .014 \quad (\text{keV-b}) \qquad \text{(II-50)}$$

We compare the fitting results with the experimental data in Table II-10. The fitting curves are plotted in Fig.II-12.

If dy/dE in (II-9) can be neglected, method iii) and method i) are identical. In case of $p+^{7}Li$ reaction, dy/dE is very small and these two methods are quite similar.

Table II-10

S-Factor for $^{7}Li(p,gamma)^{8}Be$

E (keV) (c.m.)	S (keV-b) (data)		S (keV-b) (fit)	
	(gamma1)	(gamma0)	(gamma1)	(gamma0)
34.8	.972±.195	.170±.059	.940±.003	.202±.014
52	.910	.196±.039	.940±.003	.202±.014
69.6	.910	.218±.039	.940±.003	.202±.014
87	.918	.172±.016	.940±.003	.202±.014
104	1.04	.221±.026	.940±.003	.202±.014
121	.971	.221	.940±.003	.202±.014
139	.910	.220	.940±.003	.202±.014
147	.910±.130	.194±.013	.940±.003	.202±.014

Chapter III. Reactivities

1) Introduction

From the discussions in Chapter I and Chapter II, we know that the reactivity is a combination of the cross section of nuclear reaction and the Maxwellian velocity distribution. It is given by an integral (RO78):

$$\langle \sigma v \rangle = (8/\pi\mu)^{1/2}(1/kT)^{3/2}\int_0^\infty \sigma(E)\,E e^{-E/kT}dE \qquad \text{(III-1)}$$

where μ is the reduced mass of the reactants. The integral extends from E=0 to ∞ but in the present discussion we put the upper limit at 200 keV in accordance with the limits on the present experimental reasults.

The reactivity is related to the equilibrium plasma temperature through the above integral and to the reaction rate by multiplying the product of the densities of the interacting particles. Since the plasma temperature and the reaction rate are linked by the reactivity, the reactivity plays a crucial role in the plasma temperature diagnostics.

The cross section can be expressed in terms of the S-factor S(E) (equation (II-1)). So, the reactivity may be obtained by evaluating the integral (III-1) if the S-factor is known.

In this chapter, the S-factors deduced in the previous chapter are used to calculate the gamma reactivities for the $p+^{11}B$, $p+^{6}Li$ and $p+^{7}Li$ fusion reactions, and the application to the temperature diagnostics of the advanced-fuel fusion reactor systems is discussed.

2) $\langle\sigma v\rangle_\gamma$ for $p+^{11}B$

The value of the parameter b for this reaction is calculated to be $4.75(MeV)^{1/2}$ and the reduced mass is 853.9 (MeV/c^2).

i) $^{11}B(p,gamma1)^{12}C$

The reactivity is determined by the following integral:

$$\langle\sigma v\rangle = 4.79\times10^{-18}(1/kT)^{3/2}\int_0^{200} S_\gamma e^{-E/kT-4.75/\sqrt{E}}dE \qquad \text{(III-2)}$$

where the units of the reactivity are cm^3/sec and kT is in MeV.

From Chapter II, we have:

$$S_\gamma = -.0516+.69E+2.71\times10^{-5}/((E-.15)^2+7.29\times10^{-6}) \qquad \text{(III-3)}$$

Combining (III-2) and (III-3) together, we can calculate $\langle\sigma v\rangle$ numerically. From the equation (A-1) in Appendix A, the plasma temperature kT=0 to 25 keV roughly corresponds to the Gamow energy interval 0 to 200 keV. The energy integral is evaluated over the energy integral from 0 to 200 keV,

since it is assumed that the gamma S-factor is applicable in the vicinity of the energy range of the present measurement (E(c.m.)=80-160 keV). The reactivity $\langle\sigma v\rangle$ is expressed as a function of the plasma temperature. The result is plotted in Fig.III-1.

ii) $^{11}B(p,gamma0)^{12}$

Similarly, the reactivity for the reaction $^{11}B(p,gamma0)^{12}C$ is calculated by using the gamma S-factor found in Chapter II within the same temperature range. By using the S-factor given by Davidson, the alpha reactivity is also calculated. The results are shown in Fig.III-1. The comparision between the alpha and gamma reactivity indicates that the alpha particle branch dominates the $p+^{11}B$ reaction.

3) $\langle\sigma v\rangle_\gamma$ for $p+^{6}Li$

From Chapter II, S-factor for the gamma branch is fitted to:

$$S_\gamma = 3.54\times10^{-4}E+.06 \quad (keV\text{-}b) \qquad (III\text{-}4)$$

The reduced mass for this reaction is 798.4 (MeV/C^2) and the b value is 87 $(keV)^{1/2}$. The expression for the gamma reactivity is:

$$\langle\sigma v\rangle_\gamma = 1.79\times10^{-17}(1/kT)^{3/2}\int_0^{200} S_\gamma e^{-E/kT-87/\sqrt{E}}dE \qquad (III\text{-}5)$$

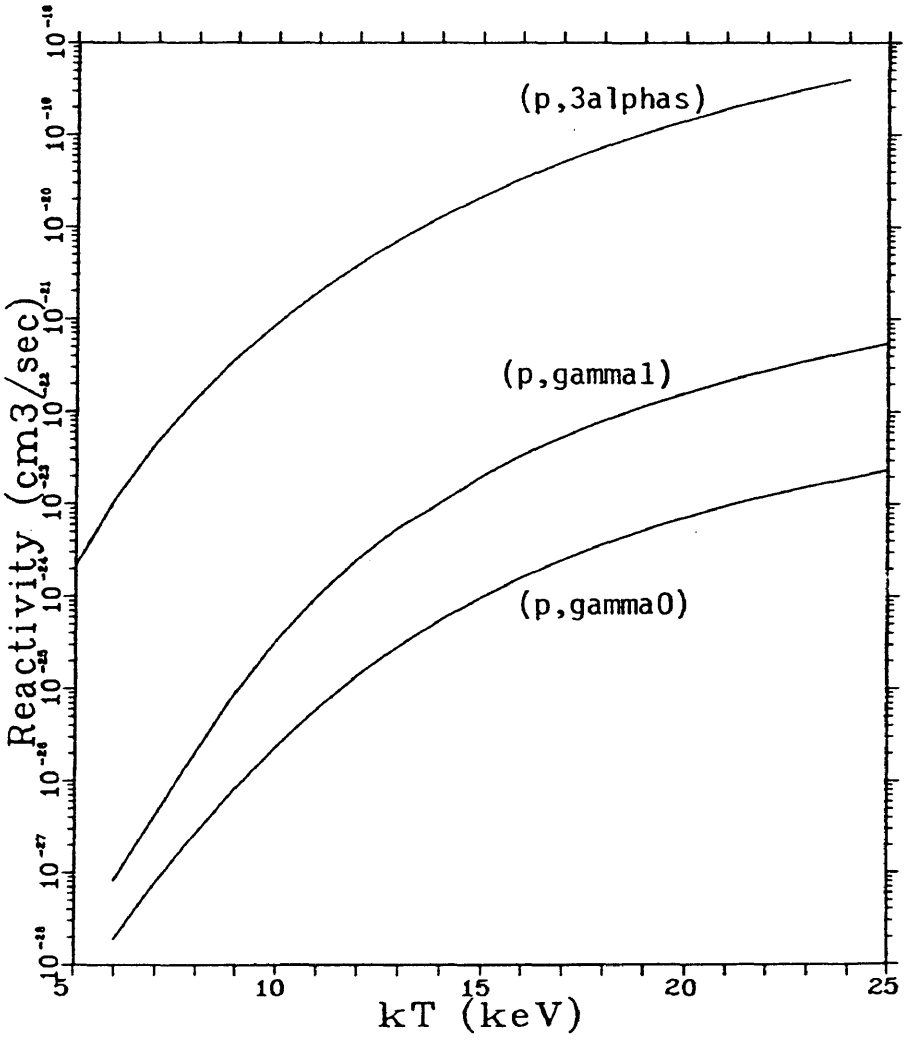

Fig.III-1. Reactivities for $^{11}B(p,3alphas)$, $^{11}B(p,gamma1)^{12}C$ and $^{11}B(p,gamma0)^{12}C$.

For the reaction p+^{6}Li, the plasma temperature kT varies from 0 to 50 keV, approximately corresponding to the Gamow-energy range of 0 to 200 keV.

The numerical calculation of gamma $\langle\sigma v\rangle$ and the comparision with the alpha $\langle\sigma v\rangle$ are presented in Fig.III-2.

4) $\langle\sigma v\rangle_\gamma$ for p+^{7}Li

The reduced mass for p+^{7}Li reaction is 815 (MeV/c^2) and the parameter b has the value of 88 (keV)$^{1/2}$.

i) ^{7}Li(p,gamma1)^{8}Be

In Chapter II, S(gamma1) was fitted to a constant (II-34):

$$S(\text{gamma1}) = .94 \text{ (keV-b)} \qquad \text{(III-6)}$$

The reactivity for the reaction ^{7}Li(p,gamma1)^{8}Be is given by:

$$\langle\sigma v\rangle = 1.77\text{x}10^{-17}(1/kT)^{3/2}\int_0^{200} .94e^{-E/kT-88/\sqrt{E}}dE \qquad \text{(III-7)}$$

ii) ^{7}Li(p,gamma0)^{8}Be

S(gamma0) was fitted to a conatant in Chapter II (II-35):

$$S(\text{gamma0}) = .202 \text{ (keV-b)} \qquad \text{(III-8)}$$

The reactivity for this reaction is found to be:

$$\langle\sigma v\rangle = 1.77\text{x}10^{-17}(1/kT)^{3/2}\int_0^{200} .202e^{-E/kT-88/\sqrt{E}}dE \qquad \text{(III-9)}$$

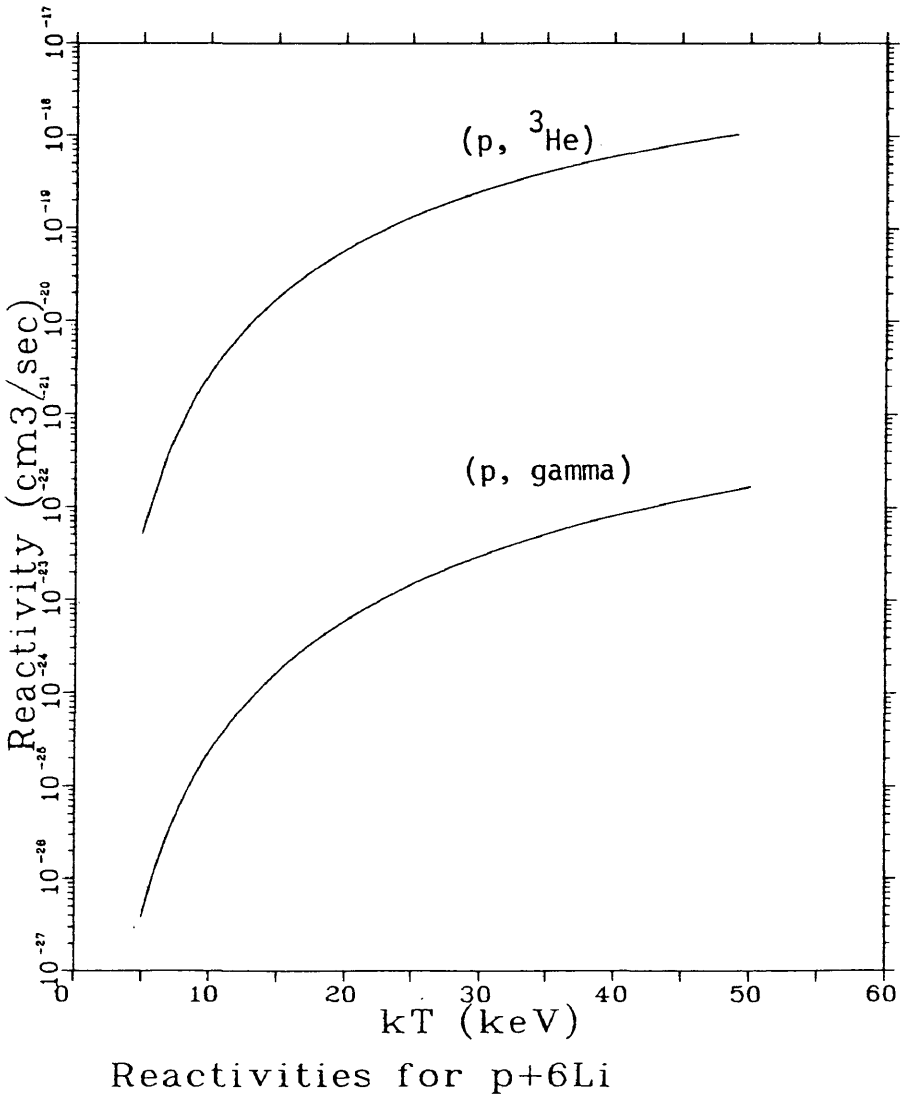

Fig.III-2. Reactivities for $^{6}Li(p,^{3}He)^{4}He$ and $^{6}Li(p,gamma)^{7}Be$

As treated for the reaction p+^{6}Li,it is reasonable for these reactivities to be evaluated as functions of plasma temperature in the range of kT=5 to 50 keV. The results of numerical calculation for the gamma reactivity and the alpha reactivity are plotted in Fig.III-3. All the gamma reactivities for these reactions are put together in Fig.III-4.

5) Application as temperature diagnostics

As introduced in Chapter I, one advantage of the advanced fuels is the fact that there are few neutrons produced in the fusion reactions. But in terms of the diagnostics of these reactor systems, the lack of neutrons actually constitutes a disadvantage since the primary reaction products will be confined in magnetic confinement systems. Fortunately, the gamma rays from the capture reactions will escape the plasma and may serve as straightforward plasma temperature diagnostics (CE87).

The effectiveness of temperature diagnostics for a fusion reactor depends upon the ability to detect an adequate number of gamma rays in a short confinement time. To obtain sufficient gamma yields, the parameters of a fusion reactor system , such as the number density of the

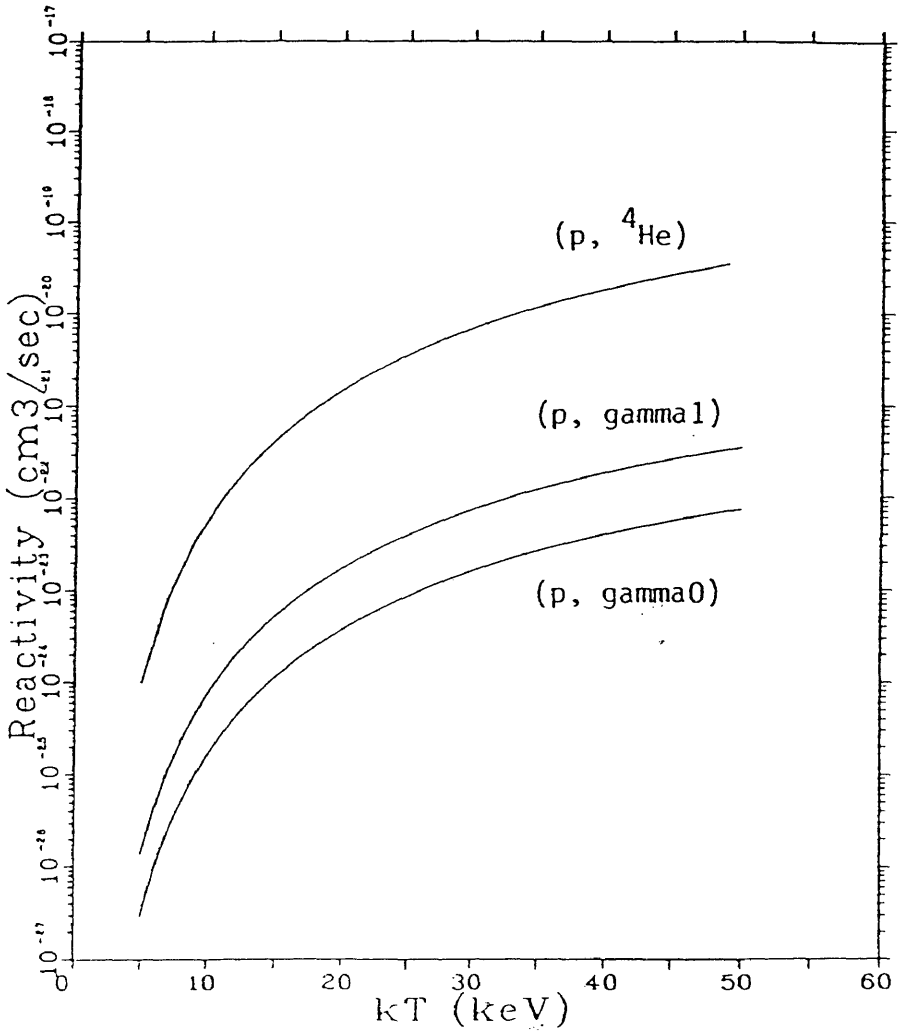

Fig.III-3. Reactivities for $^{7}Li(p,^{4}He)^{4}He$, $^{7}Li(p,gamma1)^{8}Be$ and $^{7}Li(p,gamma0)^{8}Be$.

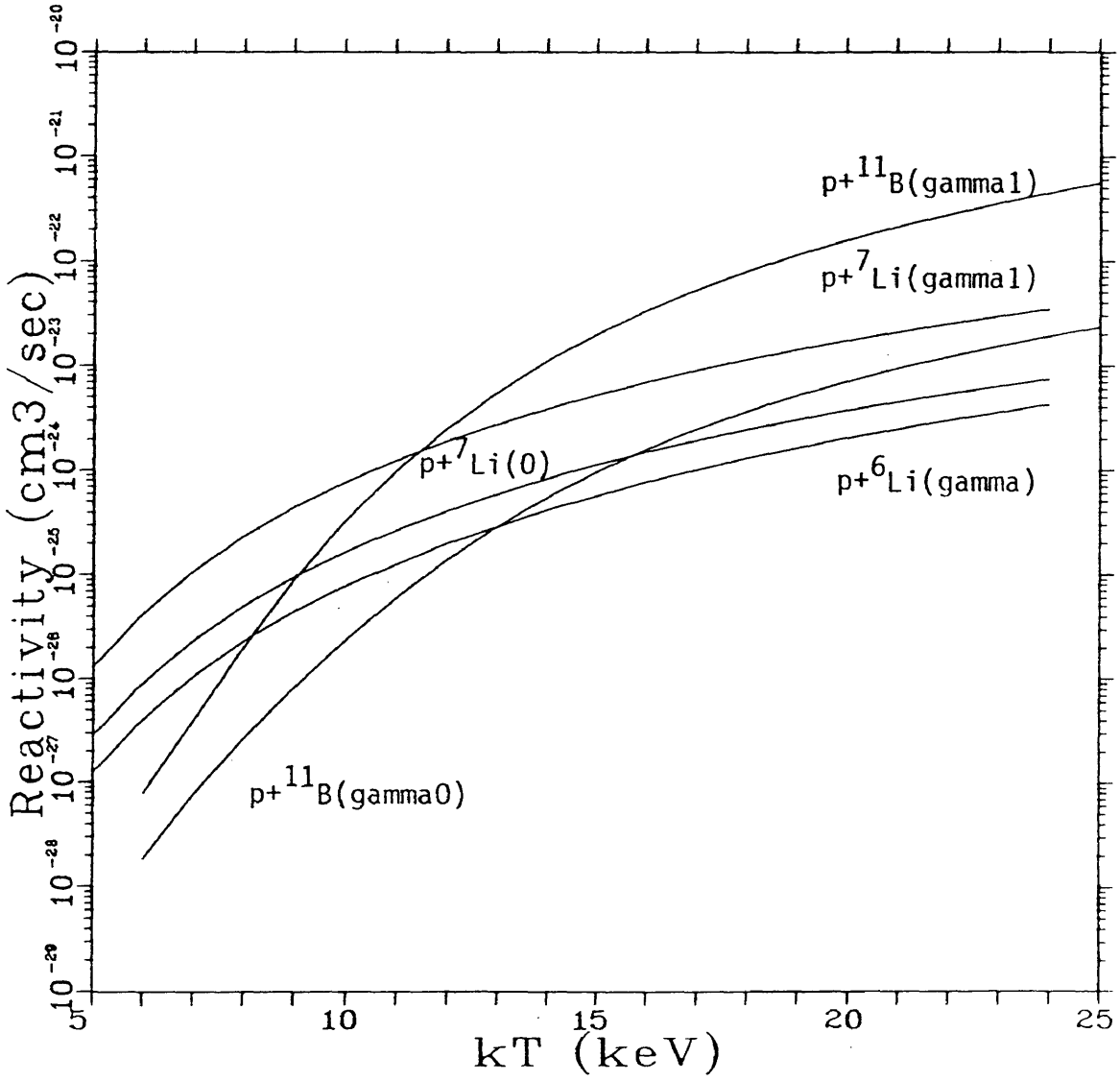

Fig.III-4 The gamma reactivities for $p+^{11}B$, $p+^{6}Li$ and $p+^{7}Li$ reactions.

plasma reactants, the volume of plasma as seen by the detector and the detector efficiency, should be properly prepared.

The expected fusion reactor might have a Tokomak design. The detection system for the Tokomak Fusion Test Reactor (TFTR) at Princeton University is shown in Fig.III-5 (CE89).

The total number of gammas produced per unit volume per unit time is (TE81):

$$R = n_1 n_1 \langle \sigma v \rangle_\gamma \qquad \text{(III-10)}$$

where n_1 and n_2 are the number densities for the proton and the target reactant, and $\langle \sigma v \rangle$ is the gamma reactivity.

The detected gamma count rate for the fusion reactor indicated in Fig. III-1 is (ME84):

$$Y_\gamma = R d\Omega / 4\pi \epsilon V e^{-\xi \eta t} \qquad \text{(III-11)}$$

where $d\Omega/4\pi=(r/2D)^2$ is the solid angle subtended by the gamma ray detector and r is the radius of the NE226 gamma detector and D is the distance from the detector to the fusion plasma; ϵ is the efficiency of the detector and V is the volume of the plasma being observed; ξ is the mass attenuation coefficient for gamma rays in the steel plate on the reaction port (as marked in position K in Fig.III-5); η is the standard density of steel and t is the thickness of steel plate. If we choose a NE226 detector with a radius

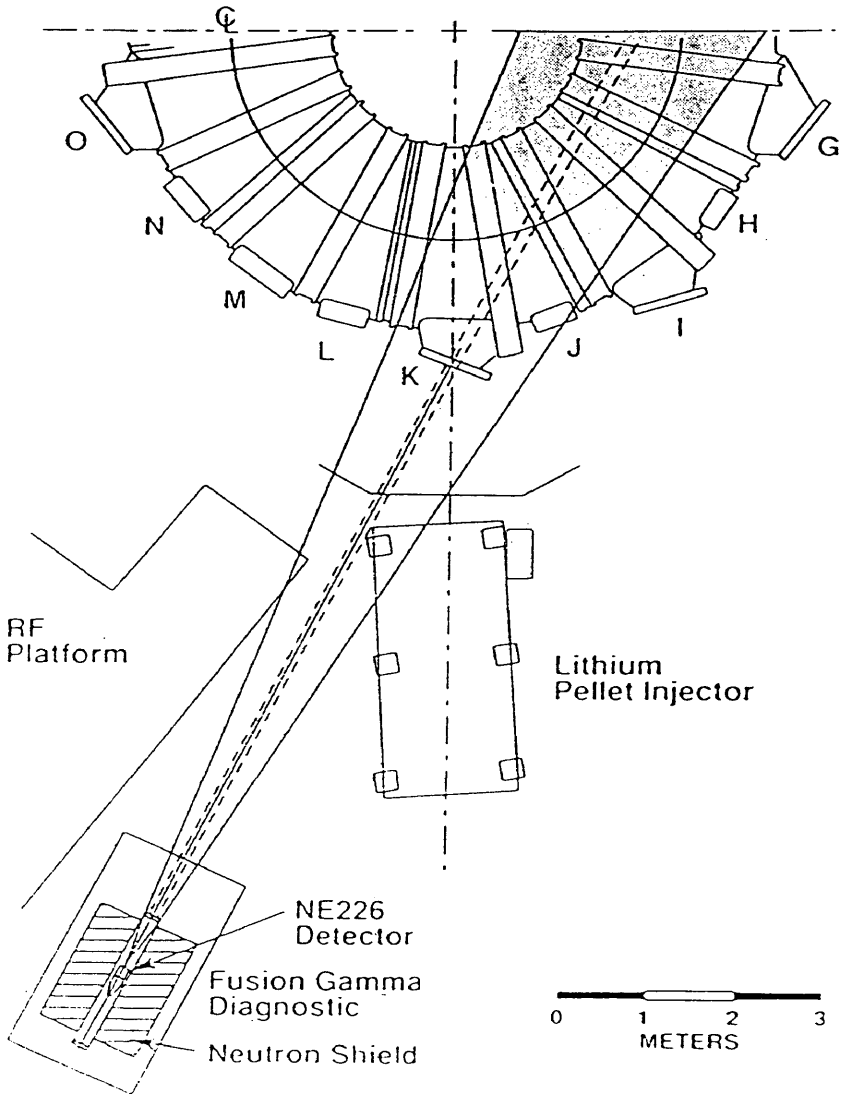

Fig.III-5. The detecting placement for gamma ray measurement on TFTR (CE89).

r=6.35 cm to detect the gamma rays and set it at a distance of about 7.5 m from the reaction port, the solid angle can be calculated:

$$d\Omega/4\pi = (r/2D)^2$$
$$= (6.35/1500)^2$$
$$= 2.06\times10^{-5} \text{ (steradians)} \qquad \text{(III-12)}$$

For our choice, the thickness of the steel plate is 3 cm, and the mass attenuation coefficient ξ for the gamma rays in steel is approximately .03 cm^2/g. The density of steel is taken to be 8 g/cm^3. The relationship between the detection efficiency of the NE226 detector and the gamma ray energy was established by Medley et al (ME84). The detection efficiencies for the studied reactions are found to be:

Table III-1

Reaction	Gamma ray energy (MeV)	Efficiency (%)
$^{11}B(p,\gamma_1)^{12}C$	11.7	6.3
$^{11}B(p,\gamma_0)^{12}C$	16.1	7.2
$^{6}Li(p,\gamma)^{7}Be$	5.6	5.3
$^{7}Li(p,\gamma_1)^{8}Be$	15.0	7.0
$^{7}Li(p,\gamma_0)^{8}Be$	18.0	7.8

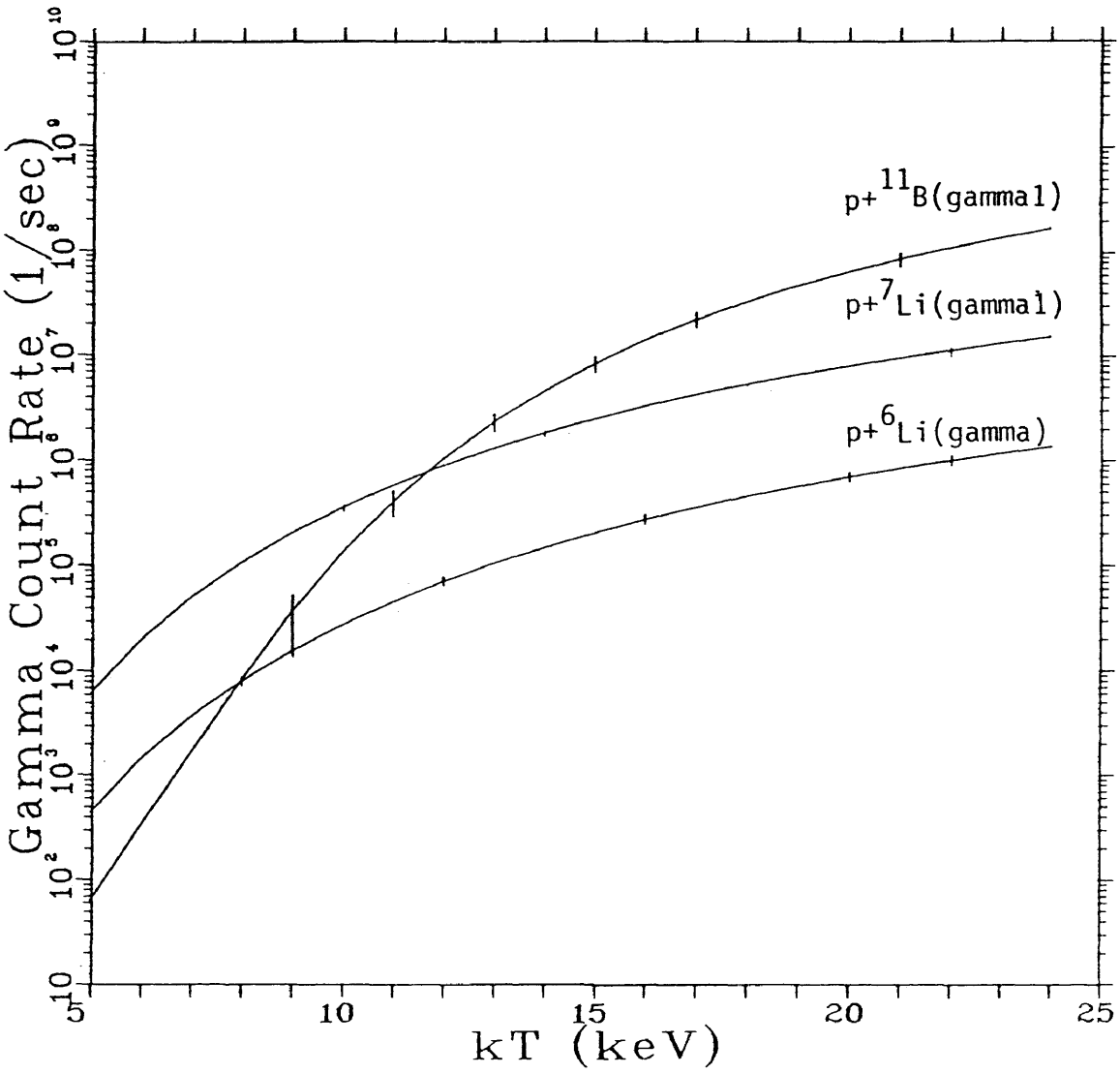

Fig.III-6 Estimated gamma ray count rates for the diagnostic placement indicated in Fig.III-1 as a function the plasma temperature ($n_p=10^{15}$, $n_B=n_{6Li}=n_{7Li}=10^{14}$ cm^{-3}). The ranges of uncertainty are presented by the error bars.

The internal radius and the external radius for the torus of the reactor indicated in Fig.III-5 are 2 m and 3 m, respectively. The volume of the fusion plasma viewed by the NE226 detector is approximately 1/3 of the torus volume:

$$V = (1/3)x500x(100^2)$$
$$= 1.64x10^8 \quad (cm^3) \qquad \text{(III-13)}$$

Now we are able to use (III-11) to estimate the gamma ray count rates for the $^{11}B(p,\gamma_1)^{12}C$, $^{6}Li(p,\gamma)^{7}Be$ and $^{7}Li(p,\gamma_1)^{8}Be$ reactions. The results are presented in Fig.III-6.

If the solid angle subtended by the detector could be enlarged, the gamma ray count rate would be increased to make up the lower gamma reactivity. And it is understandable that the larger the reaction port is, the higher the gamma count rate will be.

References

(BA74) F.C. Barker, Fifth ALNSE nuclear physics Conf., Feb. 1974, ANU Canberra, abstracts p.36.

(BI58) A.S. Bishop, "Project Sherwood-The US Program in Controlled Fusion", Addison-Wesley, 1958.

(CE84) F.E. Cecil, Nucl. Instrum. Methods A227,339(1984).

(CE85) F.E. Cecil, "Experimental Determination of the Absolute Efficiency and Energy Resolution for the NaI(Tl) and Ge(Li) Gamma Detectors at Energies from 2.6 to 16.1 MeV", Nucl. Instrum. Methods. A234, 479,1985.

(CE87) F.E. Cecil, Research Proposal to U.S. DOE, Jan.1,1987.

(CE88) F.E. Cecil, Technical Progress Report, Oct.1,1988.

(CE89) F.E. Cecil, Private communicaction.

(CL68) D.D. Clayton, "Principles of Stellar Evolution and Nucleosynthesis", McGraw-Hill, 1968.

(DA81) J.M. Dawson, "Advanced Fuel Reactors", in Fusion, Vol.1, part B. New York: Academic Press, 1981.

(DA79) J. M. Davidson, "Low Energy Cross Sections for

$^{11}B(p,3\alpha)$", Nucl. Phys. A315(1979)253.

(EL79) A. J. Elwyn, "Cross Sections for the $^{6}Li(p,^{3}He)^{4}He$ Reaction at Energies between 0.1 and 3.0 MeV", Phys. Rev. C20(1979)1984.

(FR74) H. Frauenfelder and E. M. Henley, "Subatomic Physics", New Jersey: Prentice-Hall, Inc., Englewood Cliffs, Chapter 17, "Nuclear Power".

(MA78) G. Magyar, Nuclear Fusion, 18,1978.

(ME67) W.E. Meyerhoff, "Elements of Nuclear Physics", New York: McGraw Hill, 1967.

(ME79) S.S. Medley et al, Princeton Plasma Physics Laboratory Report, TETR-TM-11, 1979.

(ME84) S.S. Medley et al, "Fusion Gamma Diagnostics", Rev. Sci.Instrum. 56(5), May 1985.

(NE84) D.E. Newman and F.E. Cecil, Nucl. Instrum. Methods. 199, 517(1984).

(RO78) C. Rolfs and H.P. Trautvetter, Annu. Rev. Nucl. Part. Sci. 28, 115(1978).

(RO86) C. Rolfs and R.W. Kavanagh, " The $^{7}Li(p,\alpha)^{4}He$ Cross Section at Low Energies", Nucl. Phys. A455, (1986)179-188.

(SW79) Z.E. Switkowski et al, " Cross Section of the Reaction $^{6}Li(p,\gamma)^{7}Be$", Nucl. Phys. A331, (1979)50-60.

(TE81) E. Teller, "Fusion, Introduction", Acedemic Press, New York, 1981.

(WA56) J.B. Warren et al, Phys. Rev. 101, 242(1956).

(WH79) C.B. Wharton, Physics Today, 5, 1979.

(YE&CE) F.R. Yeatts and F.E. Cecil, "Concepts of Physical Measurement", unpublished, 1984.

(ZE77) J.F. Ziegler and H.H. Anderson, "Hydrogen Stopping Powers and Ranges in All Elements", New York: Pergman Press, 1977

Appendix. A Reactivity

The reaction rate is the number of reactions per unit volume per unit time and is given by:

$$R=(1+\delta_{12})n_1 n_2 \langle\sigma v\rangle \qquad \text{(A-1)}$$

where is the Kronecker delta, defined as unity if the two particles are identical and as zero otherwise. The quantity $\langle\sigma v\rangle$ is the reaction rate per pair of particles and called the reactivity. It is the product of the cross section and the relative velocity, averaged over the Maxwell-Boltzmann velocity distribution:

$$\langle\sigma v\rangle = 4\pi(\mu/2\pi kT)^{3/2}\int_0^\infty v^3\sigma(v)\exp(-\mu v^2/2kT)\,dv \qquad \text{(A-2)}$$

where μ is the reduced mass for particles 1 and 2.

Nuclear reaction can proceed only when the reacting particles penetrate the repulsive Coulomb barrier that separates them. It is found that the cross section for nuclear reaction is proportional to the penetration factor:

$$\sigma(v)\propto \exp(-2\pi Z_1 Z_2 e^2/\hbar v) \qquad \text{(A-3)}$$

The penetration factor characterizes the probability for two particles of charge Z_1 and Z_2 moving with relative velocity v to penetrate their electrostatic repulsion. The quantum-mechanical interaction between two particles is inversely proportional to their relative kinetic energy E.

Therefore, the cross section can be defined as the product of three separate energy-dependent factors:

$$\sigma(E) = \frac{S(E)}{E} \exp(-2\pi Z_1 Z_2 e^2/\hbar v) \qquad \text{(A-4)}$$

The advantage of writing the cross section in this way is that two of the strong energy-dependent factors appearing in the cross section are factored out, leaving a residual function of energy, S(E), which may be very simple itself. This factor is known as the astrophysical S-factor and it represents the intrinsic parts of the nuclear cross section.

To express the penetration factor in terms of the relative kinetic energy of the two particles, we introduce the Summerfeld parameter b:

$$b/E^{1/2}=2\pi Z_1 Z_2 e^2/\hbar v \qquad \text{(A-5)}$$

The relationship between the relative velocity and energy of the particles is:

$$E=\mu v^2/2 \qquad \text{(A-6)}$$

Inserting (A-6) into (A-5), we have:

$$b=(2\pi Z_1 Z_2 e^2/\hbar)(\mu/2)^{1/2}$$

$$=31.28 Z_1 Z_2 A^{1/2} \qquad (\text{keV})^{1/2} \qquad \text{(A-7)}$$

where A is the reduced atomic weight, defined to be,

$$A=A_1 A_2/(A_1+A_2)=\mu/m_u \qquad \text{(A-8)}$$

and m_u is the mass of one atomic unit.

Consequently, the cross section can be written as:

$$\sigma(E) = \frac{S(E)}{E} \exp(-b/\sqrt{E}) \qquad \text{(A-9)}$$

Using the equations (A-6) and (A-9), from (A-2), we have the energy-dependent reactivity:

$$\langle \sigma v \rangle = (8/\mu\pi)^{1/2} (1/kT)^{3/2} \int_0^\infty S(E) \exp(-E/kT - b/\sqrt{E}) dE \qquad \text{(A-10)}$$

If the center-of-mass energy (or the relative velocity) of the pair of particles increases, according to Maxwell's velocity distribution, fewer particles will occupy the higher energy states. But the cross section deponds on the plasma energy in an opposite way: the particles with higher energy have a better chance to overcome their mutual electrostatic barrier-Coulomb barrier, compared with the others. The product of these two factors forms a compromise between the velocity distribution and the cross section. It generally has a Gaussian shape. The maximum of this Gaussian shaped curve is known as the Gamow peak (Fig. A-1). Most thermonuclear fusions take place around the Gamow peak. For this reason, this energy E_0 is frequently called the most effective energy for thermonuclear reactions. The value of E_0 is determined by the following expression:

$$E_0 = 1.22 (Z_1 Z_2 T_6) A^{1/2} \quad \text{(keV)} \qquad \text{(A-11)}$$

where T_6 is the temperature in million degrees Kelvin.

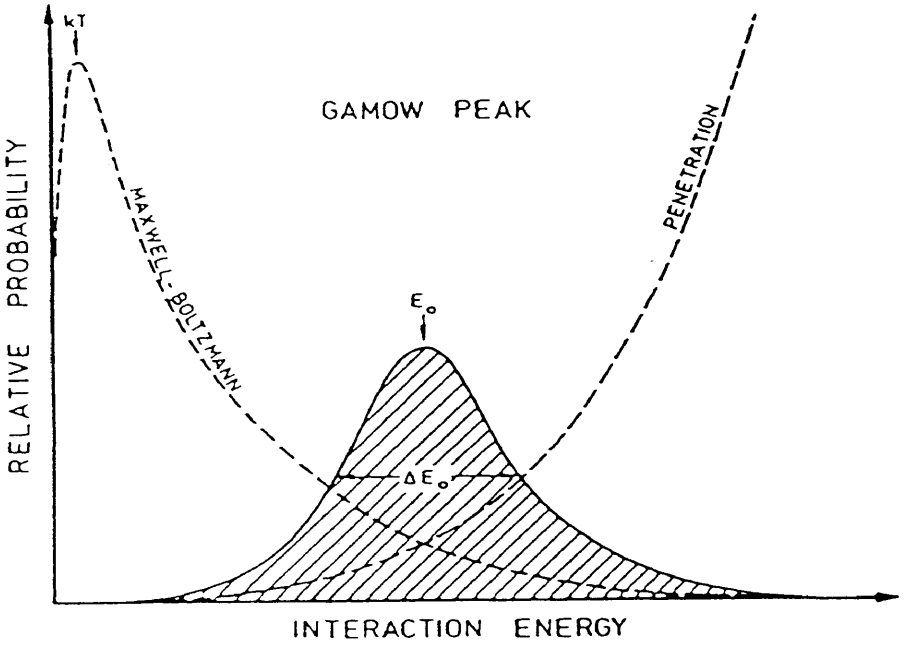

Fig. A-1 Schematic diagram of the Maxwell-Boltzmann distribution and the barrier penetration factor as a function of interaction energy. The product of these two quantities results in a Gamow peak (RO78).

Appendix. B Thick-Target Yields

The cross section for the light product in a nuclear reaction is defined as: the number of light product particles per unit time, per unit incident flux, and per target nucleus. It can be expressed as (ME67):

$$\sigma = \frac{N}{(I/A)(n)(A)(\Delta x)} \qquad \text{(B-1)}$$

where N is the number of light particles produced per unit time, I/A is the incident flux——the number of incident particles per unit time per unit area, n is the number of target nuclei per unit volume, A is the area striken by the incident beam, and Δx is the target thickness.

The expression for the gamma-ray yield per incident particle can be written as:

$$Y_\gamma = N/I \qquad \text{(B-2)}$$

From equations (B-1) and (B-2), the yield is related to the cross section as follows:

$$Y_\gamma = (\sigma)n(\Delta x) \qquad \text{(B-3)}$$

In case of thick-target reaction, the incident particles penetrate into the target by a certain depth, the expression for the yield should be adjusted to:

$$Y_\gamma = \int_0^D \sigma n dx \qquad \text{(B-4)}$$

where D is the depth which the incident particles penetrate into.

The differential change in the energy of an incident particle per differential change in depth is given by:

$$dE/dx = n\ (dE/dn') \qquad \text{(B-5)}$$

where n′ is the number of target atoms per unit area.

By using equation (B-5), we can obtain the expression written in terms of energy for the thick-target yield of gamma rays,

$$Y_\gamma = \epsilon_\gamma(E) \int_{E_0}^{0} \sigma_\gamma(E) f(E) / (dE(E)/dn) dE \qquad \text{(B-6)}$$

where $\epsilon_\gamma(E)$ signifies the detector efficiency and the solid angle subtended by the detector, f(E) is the fractional density of target atoms at a depth corresponding to an energy E_0, and the factor dE(E)/dn is known as the stopping power of the target.